NUMERICAL ELASTIC-PLASTIC ANALYSIS IN PLANE STRAIN

by

John W. Carson
B.S.M.E., Northeastern University
(1967)

SUBMITTED IN PARTIAL FULFILLMENT
OF THE REQUIREMENTS FOR THE

DEGREE OF MASTER OF SCIENCE

AT THE

MASSACHUSETTS INSTITUTE OF TECHNOLOGY

August, 1968

Signature redacted

Signature of Author . . . . . .
Department of Mechanical Engineering

Signature redacted

Certified by . . . . . .
Thesis Advisor

Accepted by . . . . . .
Chairman, Departmental Committee on Theses

NUMERICAL ELASTIC-PLASTIC ANALYSIS IN PLANE STRAIN

by

John W. Carson

Submitted in partial fulfillment of the requirements for the degree of Master of Science at the Massachusetts Institute of Technology, Department of Mechanical Engineering, 19 August 1968.

Abstract

A general program for the processing and presentation of elastic-plastic stress and strain data has been developed and applied to several plane strain problems. The program, coupled with computer-driven plotter routines, produces isoclinics, isochromatics, sliplines and/or yield zones for a given body under any loading condition. Data supplied to the program was generated by Swedlow and Yang's finite-element method and results are shown for a thick-walled cylinder loaded under internal pressure, for two notched tensile specimens (52° and 0° included angles), and for the case of a square plate with a central hole loaded under biaxial compression and tension. A user's manual for the program is also presented.

Thesis Advisor: Frank A. McClintock, Professor of Mechanical Engineering

Table of Contents

I. INTRODUCTION

The numerical stress analysis of elastic and elastic-plastic bodies is a useful tool in attempting to understand the processes of deformation and fracture. If a method could be devised whereby the manner in which a body would deform under load and also how and under what loads it would fail could be predicted, this method would be invaluable to engineering designers. Many such methods are currently being worked on and a summary of the more important ones with a tabular description of each is given in Table 1. One of the best and more easily available methods is that developed by Swedlow and Yang (1965). This program utilizes the finite-element method for an elastic-plastic body which obeys the von-Mises yield criterion and the Prandtl-Reuss flow rule. It is superior in that not only can strain-hardening be included but also an actual stress-strain curve of the material under study can be supplied to the computer. This allows for more direct comparison with experimental results. It is also possible to study the problems associated with large elastic deformations and "viscous" deformation (i.e. limit of linear hardening where the stress-strain curve has a slope of E in both the elastic and plastic regimes and Poisson's ratio is 0.5). The output from this program, while very informative, is also voluminous and difficult to analyze quickly and well. In an attempt to eaze the output analysis, a program called STANDUP (Stress Analysis of Numerical

Data Using Plotter) was developed. This program, when coupled with two computer-driven plotter routines, produces isoclinics, isochromatics, sliplines and/or yield zones for output. Program output and general analysis are presented for four different elastic-plastic bodies: thick-walled cylinder loaded under internal pressure, 52° and 0° notched tensile specimens, and a square plate with central hole loaded under biaxial compression and tension. All of these problems were run with the assumption of plane strain. A program description, sample output, and complete user's manual is presented in Appendix I.

II. REVIEW OF NUMERICAL WORK

Assembled in Table 1 are 23 different reports concerned with the static numerical analysis of various bodies. Most of the solutions listed are for elastic-plastic bodies with the exceptions of several recent works by Parmalee (1966), Wilson and Jones (1967), Speare (1968) and Butler (to be published in 1969). The various entries are arranged alphabetically by year of publication. In addition to the type of method employed, each row lists the plastic stress-strain law (flow rule), yield criterion, general assumptions (e.g. plane stress, plane strain), whether strain hardening was included ("L" means linear hardening) and examples of solutions reported. This table is not expected to be complete but rather a general description of the state-of-the-art.

As one can see, much work has been done in this field already and the solution of many practical problems (especially for aerospace work) has been attempted. Since the methods and solutions reported are so varied, little attempt has been made to correlate the results. Argyris (1965) seems to be the only one to report the solution of a three-dimensional elastic-plastic problem. No significant progress has been reported by the authors in Table 1 on a fracture criterion which could be incorporated into their results. It seems that much more work is now required in verifying experimentally and theoretically results of two-dimensional problems. Next a fracture criterion should

be adopted and checked for the simpler cases and then more attempts made to extend the programs to three-dimensions. It may turn out that the finite element technique, because of its inherent errors (explained in more detail in Section IV), will have to be abandoned and a return to some type of finite difference method considered.

III. SAMPLE PROBLEMS FROM SWEDLOW

A. Introduction

We have selected for analysis a finite element, elastic-plastic (with strain hardening) numerical program developed by Swedlow and Yang and described in references 1965, 1966, and 1968b. This program is quite general in that it can handle torsion of prismatic bars, plane stress, and plane strain problems all at a reasonable cost (e.g. $50 - $100). We have focused our attention on the last case. A multi-linear stress-strain curve can be fed into the computer, allowing for more direct comparison with experimental results. The general field equations which are applicable in their program and the specialization dictated by plane strain are described sufficiently in 1965. A description of several problems we have studied is given below.

B. Thick-Walled Cylinder.

The solution of the problem of a partially plastic thick-walled cylinder loaded under internal pressure is a classical one which has been studied by many people. Steele (1953) shows a table which compares the attempts of various authors, and he credits Sokolovsky (1943, 1946) with the only solution using von-Mises yield criterion, compressible plastic and elastic domains and strain-hardening. Mendelson (1968) also discussed the same problem and

credits Bland (1956) as the only person to include strain hardening in the solution. Both Mendelson and Bland used the Tresca yield criterion which in plane strain requires

$$\varepsilon_z^e = \varepsilon_z^p = 0$$

instead of $\varepsilon_z = 0$.

Because of the ease of applying Mendelson's results, they were employed for a comparison with Swedlow's output. All the stress variables were normalized by the uniaxial tensile strength, Y , and the radial dimensions by the inner radius of the tube. A material with relatively low strain hardening, 6061-T6 aluminum was used for the stress-strain curve. This curve is shown in Fig. 2 with the actual points supplied to the program. The applied internal pressure, p , was increased from 0.6 to 1.50 times the uniaxial tensile strength in 41 increments. Due to the symmetry of the problem, only one quadrant of the cylinder was analyzed (Fig. 4). This quadrant with an inner to outer radius ratio of 10:1 was represented by 450 triangular elements of varying size and shape; the elements were jointed at 256 nodes. Computation time on a Univac 1108 was 21 minutes (about $150).

Figure 5 shows the plastic zones (darkened areas) at various internal pressures. The criterion for deciding whether an element had yielded was the equivalent stress ($\bar{\sigma}$) divided by the equivalent stress at the proportional limit ($\bar{\sigma}_{p1}$) greater then 1.0 . This

should have given a larger plastic zone then was actually the case but Fig. 6 shows that these values of plastic zone radius, ρ_c , were actually lower than those given by Mendelson. Recall that Mendelson's equations were developed using Tresca yield and the Hencky stress-strain relations. Figures 7 to 14 compare the radial and tangential stresses versus the radius ratio for internal pressure loadings, p = 0.75, 1.00, 1.25, and 1.50 . Most seem to be in good agreement except the tangential stress in the plastic region which is probably affected by the same phenomenon as shown previously in Fig. 6. Because of low strain hardening, Mendelson's results compare almost exactly with the non-hardening results given by Hill (1950, ch. 5.2).

C. Notched Tensile Problems.

Results for two notched specimens shown in Figs. 15 and 20 loaded in plane strain tension were obtained. For each, we needed to study only one quadrant of the specimen because of symmetry. Table 2 gives the parameters for each notch. The boundary conditions for each were as follows:

$$x = 0: \quad \tau_{xy} = 0$$

$$u = 0 \qquad \text{(Horizontal displacement)}$$

$$y = 0: \quad \tau_{xy} = 0$$

$$v = 0 \qquad \text{(Vertical displacement)}$$

Figures 16 and 21 show how the plastic zone increased for each case with the same $\bar{\sigma}/\bar{\sigma}_{p1} > 1.0$ criterion as used above. At the highest load values, the axial (y-direction) strains across the neck of each specimen varied from 24% to 3% for the 52° case and 42% to 3% for the 0° case.

Figures 17 and 22 show the slip line fields for each notch specimen as drawn with the aid of VECFLD (see Appendix). The x's lie in the directions of maximum shear stress. Also shown in Fig. 17 is the non-hardening slip line field (dashed line) for a rigid-plastic notch with the same dimensions as the 52° notch after an applied stress of 2.79 times the uniaxial tensile strength on the net section. This is from Lee and Wang (1954). It seems that the "log-spiral" region persists after strain hardening but decreases in extent. We should perhaps consider this result for a minute. First of all, the equations from which the "log spiral" region are obtained are valid only for non-hardening plane strain plasticity; therefore there is no reason to expect the log spiral region to persist after hardening is introduced. On the other hand, etched deformation patterns of specimens at initial yield and at later stages of yielding (after hardening) have shown that the slip line field maintains its general shape and just expands the area of yield (see, for example, Hundy (1954)) upon straining.

After applying a stress at "infinity", the flanks of both the 52° and 0° notches remained approximately at the same angle but

the radius of curvature of the root increased. For non-hardening plasticity, an increase in flank angle would have caused an increase in "log-spiral" extent whereas an increase in root radius would have the opposite effect. Since the log-spiral region decreased in extent, this allowed for a larger constant stress region in the center which in turn allowed a greater region of yield.

Ewing (1968) restated the equations from which the plastic constraint factors for non-hardening materials could be computed. The constraint factor is the ratio of the average stress across the neck at yield to the uniaxial tensile stress. The values for the 52° and 0° notches computed from Ewing's analysis are 1.85 and 2.11 respectively. In our analysis, we took the average stress across the neck when the plastic strain increase in every element across the neck was greater than five times the elastic strain increase for two load increments (see Appendix I) and divided by the stress of 0.2% offset. The resulting values were 2.31 and 2.30. If instead of the 0.2% offset stress, the average of the stress in the most highly strained element and the proportional limit was used, the factors would have been 1.79 and 2.00 respectively which are closer to Ewing's values. At the point where these constraint factors were computed the axial strains (in the y-direction) across the neck varied from 9% to 0.6% for the 52° notch and from 16% for the 0° notch.

Pursuing Ewing's work further, we find that for both the 52° and 0° specimens their width and length were greater than the

critical values so the slip line field could be completed and didn't have to spread to the ends. Ewing also analyzed the works of Ang and Harper (1964) and Allen and Southwell (1950). He computed their constraint factors at loads where the plastic zone just touched the centerline (similar to load in Fig. 16e) and therefore got values lower than those predicted from theory. He also stated that as the load increased the plastic zone would continue into the center region but that the center itself would probably not become plastic at any finite strain. The center elements did become plastic in our case but perhaps only because of the size of the grid in that area (see Figs. 15b and 20b).

D. Square Plate with Hole Loaded in Shear.

The case of a square plate with a central hole loaded in plane strain biaxial compression and tension (or equivalently for small strains, shear at 45°) was also studied. The symmetry agreements are not as strong above (B and C) but still hold for "small" displacements. The quadrant that was studied, shown in Fig. 23, was divided into 200 triangular elements joined by 121 nodes. The boundary conditions were:

$$x = 0: \quad u = 0, \quad \tau_{xy} = 0$$

$$Y = 0: \quad v = 0, \quad \tau_{xy} = 0$$

$$X = 1: \quad \sigma_x = \sigma_{appl'd}, \quad \sigma_y = 0$$

$$Y = 1: \quad \sigma_y = -\sigma_{appl'd}, \quad \sigma_x = 0$$

A stress-strain curve for 2024-T4 aluminum (from McClintock and Argon (1966), p. 328) was used. See Fig. 3 for the curve and the points supplied to the computer. The applied stress was increased in 41 increments from 0.38 to 1.14 times the uniaxial tensile strength on the net section. Computation time on the 1108 was 5 minutes ($35).

Figure 24 shows how the yielded region progressed at several loads. The non-hardening slipline field has not been previously developed for this configuration. Figure 25 shows the VECFLD output of this slipline field. Working from this, an attempt was made to develop an admissible slip line field, but this attempt proved unsuccessful.

IV. General Prognosis of Swedlow's Program and Discussion

Based on the above presentation and experience gathered over the past year, it is worth reviewing Swedlow's program as it now stands. In its present form, the program is capable of supplying some very interesting data on many problems. We find, however, several places where the finite element technique breaks down. Figure 18 shows a VECFLD plot of the principal stresses in the lower region of the 52° notched tensile problem. Notice the tremendous jumps that are encountered in going from one row of elements to another. To give the reader an order of magnitude of the stresses involved, listed below are the various stress components (all as a fraction of the uniaxial tensile strength) of four very closely spaced elements of the 52° notched tensile specimen. These elements lie on a line normal to the free surface near the neck, are adjacent to each other, and are given in order of increasing distance from the surface. The first listed is a surface element. The applied tensile stress was 2.79 of the uniaxial tensile strength on the net section.

σ_x	σ_y	τ_{xy}	σ_z
1.62	4.81	.40	2.72
-1.16	2.58	1.17	.83
6.83	9.20	-.12	8.07
-2.70	-1.02	.23	-2.30

Swedlow (1968b) has noticed only slight changes in program output in going from a coarse to finer grid network. This has only been given a preliminary check on one problem so generalities are perhaps premature. He compared the output of the grid shown in Fig. 23 (200 elements) to that of Fig. 4 (450 elements) with both loaded far from the center hole as follows: $\sigma_x = -\sigma_y = s$. In general, the 450 element solution as opposed to the 200 element one had a smaller error and of the opposite sign when compared with the theoretical solution for an infinite plate. It was also noted that the 450 element solution, although more correct, contained more "noise" (a similar effect to that noted above. Figure 26 shows the shape of the central hole after an applied stress of 1.14 times the uniaxial tensile strength on the net section for the problem shown in Fig. 23. Supposedly it should be elliptical, but again "noise" is evident.

Some of these problems are certainly ones which are a necessary part of the finite element technqiue and no matter how fine a grid network is used, some error will always be present. It seems, however, that a judicious choice of the element shapes and distributions should have a beneficial effect on the results. The following are some guidelines which may be useful in this respect.

1) Pack small elements into regions of high strain gradients as tightly as possible (see Parmalee (1966)).
2) In regions of nearly constant stress (e.g. surface along which external load is applied), space elements uniformly.

3) Attempt to keep each pair of elements as nearly equilateral as possible. For example, elements 362 and 363 of Fig. 20a are halves of sets which are nearly equilateral. On the other hand, elements 376 and 377 show the opposite extreme which should be avoided. To show the effect, listed below are the normal strains in the y-direction for this grid with an applied stress of 3.38 times the uniaxial tensile strength on the net section. The desirability of the "square" grid is evident.

Element Number	ε_{yy}
376	.03810970
377	.03810971
378	.03142845
362	.28685578
363	.29941346
364	.25316775

The same pairing effect is shown in Figs. 8, 10, 12, and 14 for the tangential stresses in the thick-walled cylinder.

4) Try to have grid lines intersect free surfaces and center lines perpendicularly.

5) Avoid abrupt changes in grid line slopes.

6) Possibly much of the banding could be cut down by changing the grid pattern. As noted above, elements 376 and 377 in Fig. 20a are "banded" in the sense that the same strain is said to exist in each. If the grid line separating elements 377 and 378 was caused to intersect the opposite corner of this pair, perhaps the banding between 376 and 377 would be eliminated.

V. Summary and Conclusions

A data processing program has been developed and applied to the output of a finite-element, elastic-plastic stress analysis program. Three types of plane strain problems have been investigated. The case of a thick-walled cylinder loaded by internal pressure was studied because it has been solved analytically. Two notched tensile configurations (52° and 0°) and a square plate with center hole loaded in biaxial compression were looked into because of past experimental work done on these shapes.

Slipline fields were generated with the aid of the computer for all of these problems except the first one, and it was found that the field maintains its general shape after hardening is included. A critical review of the finite-element program used was also included. The biggest fault of the output seemed to be the "noise" or tremendous jumps in stress between elements and the "banding" of elements together. Several suggestions for future work follow along with a user's manual for the data processing program.

VI. Suggestions for Future Work

The following is a list of those problems the results of which would be fairly easy to obtain and very useful. Before considering specific problems, however, let us look into a normalizing scheme which has not been used but which would add greatly to the analysis effort. The following transformation is proposed:

Let $( )_{norm}$ = normalized value ,

σ_{∞} = applied stress at infinity ,

a_{net} = half-area of thinnest cross-section (e.g. Half width of neck of tensile specimen) ,

a_{gross} = half-area of largest cross-section ,

E = Young's modulus ,

Y = uniaxial tensile strength ,

then $\sigma_{norm} = \sigma/Y$,

$$(\sigma_{\infty})_{norm} = \frac{\sigma_{\infty}}{Y\left(\frac{a_{net}}{a_{gross}}\right)} ,$$

$$\varepsilon_{norm} = \frac{\varepsilon}{Y/E} ,$$

$$u_{norm} = \frac{u}{(Y/E)(a_{net})} ,$$

$$v_{norm} = \frac{v}{(Y/E)(a_{net})} \quad ,$$

$$x_{norm} = \frac{x}{a_{net}} \quad ,$$

$$y_{norm} = \frac{y}{a_{net}} \quad ,$$

then

$$E_{norm} = \frac{\sigma_{norm}}{\epsilon_{norm}} = \frac{\sigma/Y}{\epsilon/Y/E} = \frac{E}{E} = 1 \quad .$$

The advantages of such a normalization are obvious from the equations themselves.

Applying this to concrete problems, we have several which are ready to be run:

1). 90° notched tensile specimen (rounded neck) 324 elements, 190 nodes.

2). 90° notched compression specimen (sharp neck) 378 elements, 220 nodes.

3). 90° tensile specimen - square and round notches (see Joyce (1968)) round: 420 elements, 242 nodes; square: 440 elements, 252 nodes.

Looking to further program development and problem applications (see Carson (1967) and Carson and Lotz (1968)), consider the following order of priorities:

	Program Development	Problem Application	Man-hours
Mesh generation technique	X		400
Generalized plane strain	X		40
Hole growth a) Shear b) Biaxial tension		X	100
Inclusion stress		X	200
Displacement boundary conditions	X		100
Hole interaction		X	100
Low strain hardening	X		400
Instability a) Necking-buckling b) Internal		X	500-4000
Finite difference method	X		
Crack a) Mode I, II, I & II, III b) Growing (include zig-zag)		X	500-4000
Crack and hole interactions		X	
Three-dimensions	X		2000+

McClintock (1968) considers the formation of shear bands as one of the important features of ductile fracture by the growth of holes. He sets down the symmetry boundary conditions required to study a single hole under combined normal and shear displacements. This should be investigated further and incorporated into a computer run.

Acknowledgment

There are several people to whom I am deeply indebted for their helpful comments, guidance and understanding during this past year. First is my thesis advisor, Professor Frank A McClintock and second Professor J.L. Swedlow at Carnegie-Mellon University. Without them, my labors would have been much more difficult if not impossible. I am particularly grateful to Dr. Swedlow for the many days, nights and weekends he spent running programs for our use. I am also indebted to the National Science Foundation for financial support under Grant GK-1875X.

I would also like to thank my fellow graduate students, Dr. Aniruddha Chitaley, James Joyce and Jehuda Tirosh for their comments and encouragement. John Friel was extremely helpful in rewriting and polishing-up the STANDUP program, and I appreciate his fine work very much. All STANDUP runs were made at the M.I.T. Computation Center. Many thanks are also due to Sandy Williams for typing the thesis.

Finally there is one person who deserves the most thanks of all for putting up with me through this thesis program, for listening to my woes, for lifting my spirits when they were low, and for above all being a kind and loving wife. Linda has been all of these things and more to me and, therefore, to her, this thesis is dedicated.

BIBLIOGRAPHY

Allen, D.N. deG., Southwell, R.V.	1950	"Plastic Straining in Two-Dimensional Stress Systems" Phil. Trans. Roy. Soc. (London), A242, 379-414.
Ang. A., Harper, G.N.	1964	"Analysis of Contained Plastic Flow in Plane Solids", Proc. ASCE, J. Eng. Mech. 5, 397-418.
Argyris, J.H.	1965	"Continua and Discontinua", Proc. Conf. on Matrix Methods in Struc. Mech., Wright-Patterson AFB, Ohio, AFFDL-TR-66-80, 11-190.
Bland, D.R.	1956	"Elastoplastic Thick-Walled Tubes of Work-Hardening Material Subject to Internal and External Pressures and to Temperature Gradients", J. Mech. Phys. Solids 4, 209-229.
Booy, M.L.	1966	"A Non-Iterative Numerical Solution of Poisson's and Laplace's Equations with Applications to Slow Viscous Flow", ASME, J. Basic Eng., 88, p. 725.
Butler, T.G.	1969	General Purpose Program for Structural Analysis, NASA-Goddard Space Flt. Center, Md.
Carson, J.W.	1967	"Report of Discussion of Desired Program Development and Problem Applications with J.L. Swedlow", Research Memo. 125, Fatigue and Plasticity Lab., M.I.T.

Carson, J.W., Lotz, R.W. 1968 "Elastic-Plastic Problems in Fracture Research and Applications", Research Memo., Fatigue and Plasticity Lab., M.I.T.

Christopherson, O.B.E., Oxley, P.L.B., Palmer, W.B. 1958 "Orthogonal Cutting of a Work-Hardening Material", Engineering 186, 113-116.

Denke, P.H. 1956 "The Matric Solution of Certain Nonlinear Problems in Structural Analysis", J. Aero. Sci. 23, 3, p. 231.

Ewing, D.J. 1968 "The Plastic Yielding of V-Notched Tension Bars with Circular Roots", J. Mech. Phys. Solids 16, 81-98.

Fowler, J. 1967 "Elastic-Plastic Analysis of Asymmetrically Loaded Shells of Revolution", S.M. Thesis, Dept. of Aero. and Astro., M.I.T.

Gallagher, R.H., Padlog, J., Bijlaard, P.P. 1963 "Stress Analysis of Heated Complex Shapes", ARS Journal 32, 5, 700-707.

Gallagher, R.H., Padlog, J., Huff, R.D. 1964 Thermal Stress Determination Techniques for Supersonic Transport Aircraft Structures, Part III - Computer Programs for Beam, Plate, and Cylindrical Shell Analysis, Air Force Systems Command, ASD-TR-63-783.

Goldberg, J.E., Richard, R.M. 1963 "Analysis of Nonlinear Structures", Proc. ASCE, J. Struc. Div. 89, ST4, 333-351.

Hetényi, M. 1950 Handbook of Experimental Stress Analysis, John Wiley and Sons, New York.

Hill, R. 1950 The Mathematical Theory of Plasticity, Oxford University Press.

Hundy, B.B. 1954 "Plane Plasticity", Metalurgia 49, p. 293.

IBM 1967a Application Program, 1130 Numerical Surface Techniques and Contour Map Plotting (1130-CX-11X), Operator's Manual H20-0356-0.

IBM 1967b Application Program, 1130 Numerical Surface Techniques and Contour Map Plotting (1130-CX-11X), Programmer's Manual H20-0357-0.

IBM 1967c Application Program, 1130 Numerical Surface Techniques and Contour Map Plotting (1130-CX-11X), Application Description H20-0140-2.

Isakson, G., Armen, H., Pifko, A. 1967 Discrete-Element Methods for the Plastic Analysis of Structures, NASA CR-803.

Joyce, J.A. 1968 "Tensile Plastic Deformation at Notch Roots", S.M. Thesis, Dept. of Mech. Eng., M.I.T.

Jurišić, D. 1963 Two-Dimensional Elastic-Plastic Stress and Strain Analysis, Ljubljana Univ., Yugoslavia

Lansing, W., Jensen, W.R., Falby, W. 1965 "Matrix Analysis Methods for Inelastic Structures", Proc. Conf. on Matrix Methods in Struc. Mech., Wright-Patterson AFB, Ohio, AFFDL-TR-66-80, 605-634.

McClintock, F.A., Argon, A.S. (eds) 1966 Mechanical Behavior of Materials, Addison-Wesley, Reading, Mass.

McClintock, F.A. 1968 "Strain Hardening Relations and Boundary Conditions for Numerical Calculations of Plastic Flow", Fatigue and Plasticity Lab., M.I.T.

Mendelson, A.	1968	Plasticity: Theory and Application, The MacMillan Co., New York.
Mentel, T.J.	1966	"Study and Development of Simple Matrix Methods for Inelastic Structures", J. Spacecraft and Rockets 3, 4, p. 449.
Parmalee, R.P.	1966	"Three-Dimensional Analysis for Computer Aided Design", Ph.D. Thesis, Dept. of Mech. Eng., M.I.T.
Percy, J.H., Loden, W.A., Navaratna, D.R.	1963	A Study of Matrix Analysis Methods for Inelastic Structures, Tech. Doc. Report RTD-TDR-63-4032, Air Force Systems Command.
Pope, G.G.	1965	"The Application of the Matrix Displacement Method in Plane Elasto-Plastic Problems", Proc. Conf. on Matrix Methods in Struc. Mech., Wright Patterson AFB, Ohio, AFFDL-TR-66-80, 635-654.
Sokolovsky, W.W.	1943	"Elastico-Plastic State of a Cylindrical Tube Yielding with a Strain-Hardening of Material" (in Russian), Prik. Mat. i Mek. 7, 273-292, or "Elastic-Plastic Equilibrium of a Tube made of a Material with Strain Hardening", Brookhaven Nat'l Lab. Translation.
Sokolovsky, W.W.	1946	Theory of Plasticity (in Russian), Moscow, USSR, ch.3.
Speare, J.	1968	"Discrete-Element Static Analysis of Core-Stiffened Shells of Revolution for Asymmetric Mechanical Loading", M.S. Thesis, Dept. of Aero. and Astro., M.I.T.
Steele, M.C.	1952	"Partially Plastic Thick-Walled Cylinder Theory", ASME, J. Appl'd Mech. 19, 2, 133-140.
Stimpson, L.D. Eaton, D.	1961	The Extent of Elasto-Plastic Yielding at the Crack Point of an Externally Notched Plane Stress Tensile Specimen, ARL-TR-24, Aero. Research Lab., Wright-Patterson AFB, ASTIA-AD-266-347. Condensed in Williams, M.L., Proc. Crack Propagation Symposium, Cranfield (Eng), 1961, 130-165.

Stricklin, J.	1963	"Large Elastic, Plastic, and Creep Deflections of Curved Beams and Axisymmetric Shells", Ph.D. Thesis, Dept. of Aero. and Astro., M.I.T.
Swedlow, J.L., Williams, M.L., Yang, W.H.	1965	"Elasto-Plastic Stresses and Strains in Cracked Plates", Proc. 1st Int'l Conf. on Fracture (Sendai) 1, 259-282.
Swedlow, J.L. Yang, W.H.	1966	Stiffness Analysis of Elasto-Plastic Plates, Air Force Rocket Propulsion Lab., Edwards AFB, AFRPL-TR-66-5.
Swedlow, J.L.	1968a	Personal communication.
Swedlow, J.L.	1968b	"Character of the Equations of Elasto-Plastic Flow in Three Independent Variables", Int'l. J. Nonlinear Mech.
VECFLD	1968	User's Manual, by J. Carson, G. Hornik and S. Madnik, Research Memo., Fatigue and Plasticity Lab., M.I.T.
Wilson, E.L.	1960	"Matrix Analysis of Nonlinear Structures", Second Conf. on Elec. Comp., Pub. by ASCE, 415-428.
Wilson, E.L., Jones, R.M.	1967	Finite Elastic Stress Analysis of Axisymmetric Solids with Orthotropic Temperature-Dependent Material Properties, Air Force Report No. BSD-TR-67-228, Aerospace Report No. TR-0158-(S3816-22)-1.

APPENDIX I.

DATA PROCESSING PROGRAM

A. Introduction

This Appendix is intended to be self-contained as a user's manual for STANDUP (STress Analysis of Numerical Data Using Plotter). First this data processing program will be described in general terms as to what it can do. Next we will list the specific input data required and in what order it must be added. Several references are made to locations within the program deck for use on an IBM OS/360-65 computer on which this has been run. This program which is written in Fortran IV-G should be operable on other computers of comparable size. Computer storage required is about 200,000 bytes (or 1,600,000 bits). Execution time is of the order of two minutes CPU time. The program has been liberally interspersed with comment cards to aid in future additions or changes to the program. Output has been designed to be self explanatory. It lists all the input data used in the computations and all the output data punched.

Flow charts are also given below for the main sub-routines of the program. Those for which flow charts are not given are merely sub-routines which call others for execution purposes or which read data. A program and data set flow chart is shown in Fig. A-1 which describes the interactions between STANDUP, the output plots, and a source (stress analysis data) program.

B. General Description

The data processing program (STANDUP) is set up to perform several manipulations of numerical stress analysis data to be able to analyze the data more efficiently and meaningfully. The basic input data consists of the values of a multilinear stress-strain curve, the values of the displacements and final coordinates of each nodal point, and the stresses (σ_x , σ_y , τ_{xy} and σ_z) and strains (ε_x , ε_y and γ_{xy}) for each element under a given applied stress. All the input required is listed in more detail later.

Since STANDUP only supplies punched and printed output, it was desirable to put this output in such a form that some computer plotting routines could be employed. The two most useful such routines are VECFLD ("Vector Field") and CONTR ("Contour"). VECFLD (1968), a program developed by Stuart Madnik and later revised by the author and Digital Programming Services, Inc., accepts the coordinates of up to 999 random data points and the x - and y - components of up to five vectors at each point. It connects the points to draw a grid and/or plots the vectors at each point. It is set up presently for IBM OS/360 and the CalComp plotter.

CONTR (IBM-1967a,b,c) is an IBM-supplied disk for the 1130 computer with associated plotter. It accepts the coordinates of up to 1599 random data points and the value of some parameter at each point (e.g. elevation above sea level, temperature) and draws lines of constant value ("contours") through the region. Listed below are

the various subprograms of STANDUP which can be called to be performed:

1. List. This subprogram takes the data which is supplied to it and performs various computations so that the output is similar to the regular output listing supplied by J.L. Swedlow. This output, in addition to the rewritten input data consists of the following variables: ε_x^p , ε_y^p , γ_{xy}^p , ε_z^p , elastic dilatation $(\varepsilon_x^e + \varepsilon_y^e + \varepsilon_z^e)$, σ_x/Y , σ_y/Y , τ_{xy}/Y , σ_z/Y , equivalent stress $(\bar{\sigma})$ / equivalent stress at proportional limit $(\bar{\sigma}_{pl})$, γ_{max} , γ_{max}^p , equivalent strain $(\bar{\varepsilon})$, $\bar{\varepsilon}^p$, τ_{max} , $\bar{\sigma}$, and strains normalized with respect to the strain at the proportional limit. Superscripts "e" and "p" stand for the elastic and plastic parts.

2. Isoclinics. Recorded experimentally in photoelasticity studies, these are lines of constant principal stress direction. This subprogram is set up such that the values of angles of principal stress directions are punched out for each element along with the coordinates of the "point" where each value is computed. The option is available to compute these coordinate values for either the standard x-y plane or for a transformed i-j plane where all the columns and rows of the grid network are replaced by straight lines. These values can be supplied to CONTR to draw the isoclinics.

3. Isochromatics. Like isoclinics, these are also observed experimentally in photoelastic studies. They are lines of constant difference of principal stress (i.e. $\sigma_1 - \sigma_2$ = constant). This subprogram is set up to punch out the values of this principal stress difference (or principal strain difference, if desired) along with either the x-y or i-j coordinates of each "point" as above. These values can be supplied to CONTR to draw the isochromatic contours.

4. Sliplines. In order to calculate the external loads needed to cause deformation within the plastic region of a plane strain body, it is necessary to know the variation in the mean compressive stress, p , within that region. The solution is obtained by constructing a slip-line field, the lines of which are parallel to the orthogonal directions of maximum shear stress within the plastically deforming region of the body. These slip-lines are also directions of zero normal strain rate, i.e. there is no change in length along these lines. It also turns out that in non-hardening plasticity they are the characteristics of the hyperbolic plane strain equations (found by differentiating the yield criterion) and that along one line (the α - line)

$$p + 2k\phi = \text{constant}$$

and along another (β) line,

$$p - 2k\phi = \text{constant}$$

where k = maximum shear stress

ϕ = counterclockwise angular rotation of the α-line from the x-axis.

In our case, we were able to obtain the slipline fields, since we already knew p and ϕ ; we wished therefore to work back from this to be able to visualize the flow fields and also to investigate the usefulness of non-hardening slipline fields after hardening has ensued. This subprogram punches out the x - and y - components of a unit vector in the directions of maximum shear stress for the centroid of each element. These can be supplied to VECFLD to draw the maximum shear directions. In addition, the values of the quantities $p + 2k\phi$ and $p - 2k\phi$ are punched out to be supplied to CONTR. For an elastic-plastic stress analysis which includes strain hardening, the values of the constants along the characteristics should more properly be (Christopherson et. al., 1958)

$$p + 2k\phi - \int \frac{dk}{ds_\beta} ds_\alpha = \text{constant along } \alpha\text{-line}$$

$$p - 2k\phi - \int \frac{dk}{ds_\alpha} ds_\beta = \text{constant along } \beta\text{-line}$$

where ds_α and ds_β are increments along the α - and β - lines. Since these integrals are difficult to evaluate in our case, we will ignore them and contour only $p \pm 2k\phi$. The

resulting contour map was of little usefulness but the VECFLD output was very helpful in approximating the non-hardening slip-line field.

5. Yieldzone. The fact that a particular "point" or element has been stressed above the proportional limit is not a completely valid criterion as to whether the "point" is continuing to yield plastically or not. Because of this, this subprogram compares the increases in axial strain (in direction of loading) to some constant times the elastic strain increment (i.e. stress increment divided by Young's Modulus). If the total increase is greater than the elastic increase, the value of 1.0 is punched for that point; otherwise a 0.0 is punched. This can then be supplied to CONTR to get the region of yield.

C. Input Data

The following pages define the input data required for STANDUP. There are three types of data cards; each is explained in more detail in the following paragraphs.

A). Special Data Card, DATA CARD 1.

This special program data card, labeled in the upper right corner as DATA CARD 1, is suppliedwith the program and must not be altered in any way. It must be the first card in any data set. On the OS/360, it must follow immediately after the //G.SYSIN DD * card.

B). Command and Control Cards.

The following is a listing of command and control cards for sequencing operations and the format in which they must be typed:

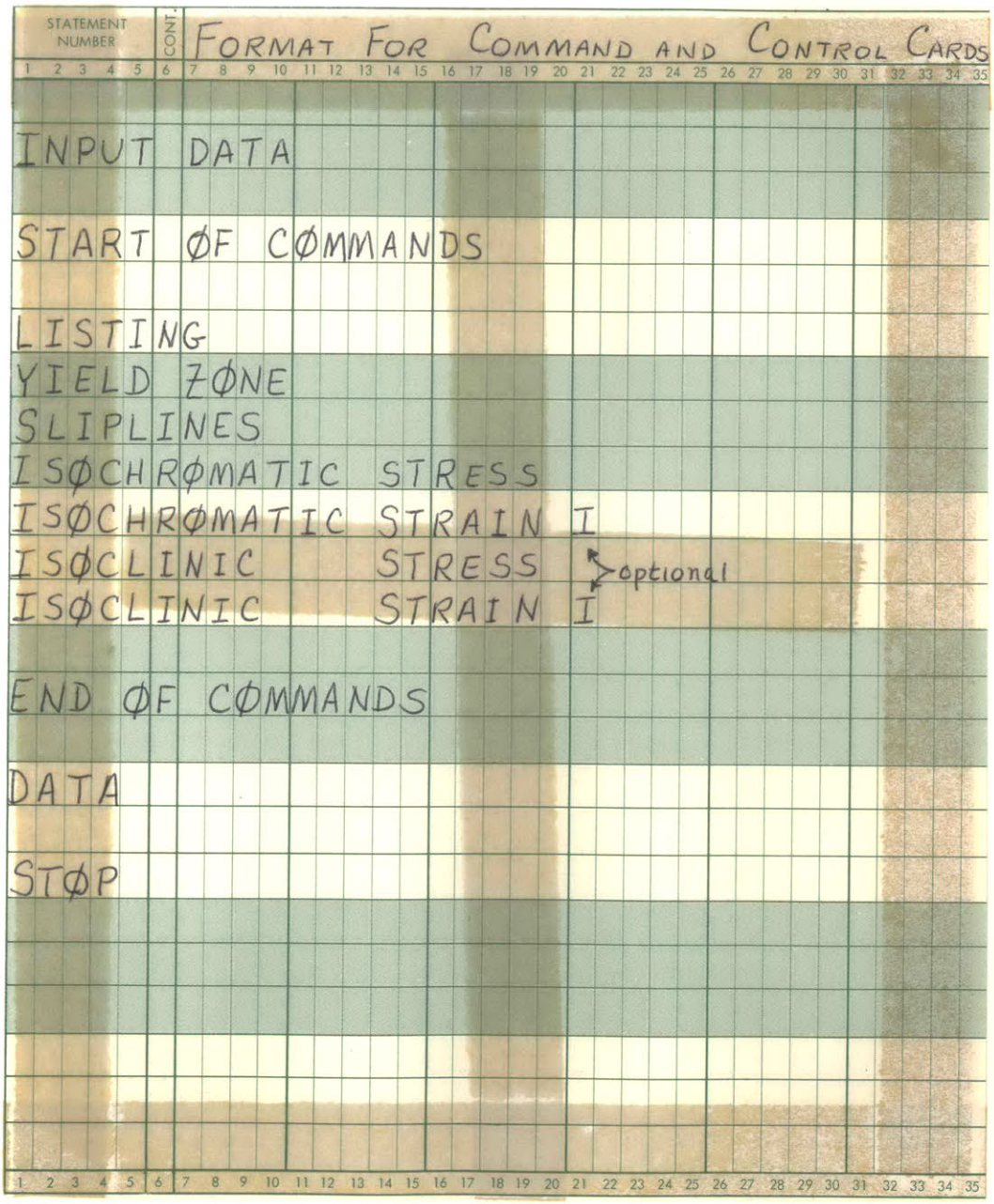

C). Numerical Input Data.

All user supplied numerical input is of three types:

I Integer, no decimal point, right-justified.

F Real number, must include decimal point. This may be located anywhere in the field specified (e.g. 3260.) .

A Any alphanumeric characters for title purposes.

The numerical input for STANDUP falls into four main categories:

1). Input Data Set

These cards follow immediately after the command card INPUT DATA, and for any run there must be one INPUT DATA command card and one Input Data Set immediately after DATA CARD 1. Other Input Data Sets may be furnished in the succeeding data sets if desired in a given run. The following cards comprise the Input Data Set:

Order	Information	Type	Columns
1	Title	A	1-72
2	Two times the maximum difference between nodal numbers for a given element +4	I	1-3
	Two times the number of nodal points	I	5-7
	The number of elements	I	9-11

Order	Information	Type	Columns
	The number of points on the stress-strain curve	I	13-15
	The number of displacement boundary conditions (u or v = 0)	I	17-19
	The number of stress load increments	I	29-31
3	Young's modulus	F	1-20
	Poisson's ratio	F	21-40
4	Multi-linear stress-strain curve values - one stress-strain set per card:		
	octahedral plastic strain (1)	F	11-30
	octahedral shear stress (1)	F	31-50
5	Displacement boundary conditions for u or v = 0 . For v = 0 , take nodal number and multiply by two. For u = 0, take nodal number, multiply by two and subtract one. (Eighteen values to a card and a total number of values as specified above)	I	1-3 5-7 9-11 . . 69-71

Order	Information	Type	Columns
6	Stress load increment values (nine values to a card and a total number of values as specified above)	F	1-8 9-16 . . 65-72
7	Values of nodal numbers associated with each element (3 per element counterclockwise) in numerical order of elements.	I	1-3 4-6 7-9 . . 67-69
8	Initial coordinates of nodal points - one set of x-y points per card:		
	x_i	F	11-30
	y_i	F	31-50

2). Load Increment Specification Set

This set must follow the control card DATA every time it is used. Consisting of two or more cards, this set supplies information as to how many Load Increment Sets will follow, how many of those are to be read, and their increment numbers.

Order	Information	Type	Columns
1	Number of Load Increment Sets to be read	I	1-3
	Number of Load Increment Sets to be supplied in the following increment set	I	5-7
2	The load increment numbers of the data sets to be read, maximum of 20 per card and fill as many cards as needed	I	1-3 5-7 9-11 . . 77-79

3). Load Increment Set.

These sets usually follow the Load Increment Specification Set; however, with the command YIELD ZONE, one Load Increment Set appears without a Load Increment Specification Set. The setup of this is as follows:

Order	Information	Type	Columns
1	Applied stress load	F	1-10
	Total elastic energy	F	11-30
	Total plastic work	F	31-50
	Total work	F	51-70
	Load increment number	I	76-77

Order	Information	Type	Columns
2	X-displacement of node	F	1-8
	Y-displacement of node	F	9-16
	Final x-coordinate of node	F	17-23
	Final y-coordinate of node	F	24-30
	ε_{xx}	F	31-37
	ε_{yy}	F	38-44
	γ_{xy}	F	45-51
	σ_{xx}	F	52-57
	σ_{yy}	F	58-63
	τ_{xy}	F	64-69
	σ_{zz}	F	70-75
	Load increment number	I	76-77
	Node or element number	I	78-80

The above format for the second card is used until the displacements and coordinates of all the nodal points has been satisfied. Since for Swedlow's grid, the number of nodal points is always less than the number of elements, the stresses and strains of the remaining elements must be supplied. Their format is as follows:

Order	Information	Type	Columns
3	ε_{xx}	F	1-10
	ε_{yy}	F	11-20
	γ_{xy}	F	21-30

Order	Information	Type	Columns
	σ_{xx}	F	31-40
	σ_{yy}	F	41-50
	τ_{xy}	F	51-60
	σ_{zz}	F	61-70
	Load increment number	I	76-77
	Element number	I	78-80

4). Additional Numerical Input Set

Certain commands require additional data to follow each Load Increment Set which follows a DATA card and a Load Increment Specification Set. It is possible with this program to omit in certain instances the DATA card and Load Increment Set entirely for the given command if the Load Increment Set of the previous command is to be reused. In this event, a blank card follows the command, and the additional data (if it is required) must follow the blank card. Listed below are the various subprograms which require additional data and an explanation of what that data consists.

YIELD ZONE - This requires an additional Load Increment Set which can be either for a previous or succeeding load increment to the one in question. This additional

Load Increment Set has no Load Increment Specification Set with it, and it is not included in any previous Specification Set.

SLIPLINES - One card containing the value for the maximum shear stress must follow each Load Increment Set on which slipline field calculations are performed. This value is Type F and in column 1-15. If it is desired to have the program compute an "average" value of the maximum shear stress, this card must still be supplied but is completely blank.

ISOCHROMATICS/ISOCLINICS VARIATION I - Variation I is an option that can be called with isochromatics or isoclinics by placing an I in Column 21 of the Command Card. If this option is not desired, Column 21 is simply left blank. This option calls the subroutine CENTRI instead of CENTRX and in doing so computes the centroids of a transformed I-J plane where all the rows and columns of the grid are replaced by straight lines. The total number of rows and columns (both including ends) must be supplied. They follow each Load Increment Set, are Type I variables, and are located in Columns 1-3 and 5-7 respectively.

The Complete Data Package.

STANDUP is unique in that it allows not only the execution of a given command on a sequence of Load Increment Sets but also sequencing of various commands on a number of Load Increment Sets and even the execution of commands on load increments from two or more different specimens.

Organization of the Data Package.

The complete data package must always begin with the following sequence of cards. Note that in the following information, words which must physically occupy the card are all in capital letters (e.g. INPUT DATA) whereas other information referring to sets of data (e.g. Input Data Set) are not.

Order	Information
1	(Data Card 1)
2	INPUT DATA
3	(Input Data Set)
4	START OF COMMANDS

After the START OF COMMANDS card, the sequence for the remainder of the data package is determined by the user's needs. If the user wished to operate on a single Load Increment Set, he would use the following order after the START OF COMMANDS card:

Order	Information
5	(Sample Command) e.g. SLIPLINES

Order	Information
6	DATA - The first Command Card must be followed by a DATA card, a Load Increment Specification Set, and at least one Load Increment Set.
7	(Load Increment Specification Set - specifying one set to be read, one to be supplied, and the increment number)
8	(Load Increment Set)
9	(Additional Numerical Input Set if needed for this command)
10	STOP
11	END OF COMMANDS

Please note that the STOP card must preceed every additional Command Card except for the command following a START OF COMMANDS card. The END OF COMMANDS card must be at the physical end of the data package. On OS/360 it precedes the final /* card.

To run one command on a sequence of load increment sets, the data set package after the START OF COMMANDS card would be organized this way:

Order	Information
5	(Sample Command) e.g. YIELD ZONE
6	DATA
7	(Load Increment Specification Set)
8	(First Load Increment Set)

Order	Information
9	(Additional Numerical Input Set - if necessary)
	Repeat (8) and (9) as many times as desired.
10	STOP
11	END OF COMMANDS

Running a sequence of various commands on one or more Load Increment Sets is possible through the following sequence after the START OF COMMANDS card:

Order	Information
5	(Sample Command 1) e.g. ISOCLINICS
6	DATA
7	(Load Increment Specification Set)
8	(Load Increment Set)
9	(Additional Numerical Input Set - if necessary)
	Repeat (8) and (9) as desired
10	STOP
11	(Sample Command 2) e.g. LISTING
12	DATA
13	(The (7),
14	(8),
15	(9) sequence as above)
16	STOP
17	(Sample Command 3) e.g. YIELD ZONE

Order	Information
18	(Blank Card) Note: Use of the blank card instead of a DATA card causes the command to be executed using the last Load Increment Set read into the machine.
19	(Additional Numerical Input Set - if needed)
20	STOP
21	END OF COMMANDS

The fourth key user option is that of using Load Increment Sets from two or more specimens. The sequence for this is straightforward. Commands are sequenced for the first specimen; then, immediately following the last STOP card, an INPUT DATA card is inserted. The Input Data Set for the second specimen is then inserted. The following is an example of such sequencing:

Order	Information
1	(Data Card 1)
2	INPUT DATA
3	(Input Data Set 1)
4	START OF COMMANDS
5	(Sample Command) e.g. Sliplines
6	DATA
7	(Load Increment Specification Set)
8	(Load Increment Set)

Order		
9	(Additional Numerical Input Set - if necessary)	
10	STOP	
	(5) to (10) repeated as many times as desired	
11	INPUT DATA	
12	(Input Data Set 2)	
13	START OF COMMANDS	
	(5) to (10) sequence as above	
14	END OF COMMANDS	Note: It should be emphasized that this card appears only once at the physical end and does <u>not</u> appear between Input Data Sets.

The manner of sequencing of data should be re-emphasized. First, STANDUP will continue to use the same Input Data Set for each command until a new Input Data Set is specified (as in the last example above). In a similar fashion, STANDUP will execute with each command the Load Increment Set(s) immediately following the command (i.e. after the DATA card). Each set is read in and the preceeding one is destroyed; therefore if one wished to use the option of sequencing commands on the <u>same</u> Load Increment Set, he would do this by placing a blank card and a STOP card after the second, third, etc. command cards (note that no DATA Card is required). He must be aware that these commands will be executed on only the <u>last</u> Load Increment

Set read into the machine whether this be a specified Load Increment Set (one following a DATA card) or an Additional Numerical Input Set (the additional set needed with the command YIELD ZONE). Also note that when Additional Numerical Input Sets are required, they must be supplied after each command needing them regardless of how sequencing is done.

D). Sample Problems and Output.

In this section, several samples of the various subprogram outputs described above will be presented. All these examples are plane strain problems.

1. List. An example of the output from the List subprogram was deemed unnecessary since it is self-explanatory above.

2. Isoclinics. Most isoclinics which are experimentally obtained are done so under plane stress load conditions. The output we have available is for plane strain problems. With this in mind, consider Fig. 27 which is a CONTR plot of one set of isoclinics for the first load increment for the case of a square plate with central hole loaded in biaxial compression and tension (Fig. 23). The other set is orthogonal to this set. To the author's knowledge, this field has not been developed experimentally so no verification is possible.

3. Isochromatics. Recalling the restrictions mentioned above concerning isoclinics, Fig. 28 presents the isochromatics

for the same problem. The results are in reasonable agreement with experimental work (see, for example, Hetényi (1950), p. 855, Fig. 17-17). The input data deck to STANDUP is displayed in Table 3.

4. Sliplines. For the specimen shown in Fig. 15, the slipline field produced by VECFLD is shown in Fig. 17. Both sliplines must and do intersect the free surfaces at 45° because, by definition, a free surface has no normal or shear traction on it. The same is true for lines of symmetry because of a lack of shear stress along such lines. This slipline field is similar to that given by Lee and Wang (1954) for a rigid-plastic non-hardening material. The CONTR output of $p \pm 2k\phi$ seemed to make no sense at all.

5. Yieldzone. The arbitrary constant mentioned above by which the elastic strain increment was multiplied was set in the program to equal 5.0. Shown in Fig. 19 is the CONTR output for the specimen shown in Fig. 15. This is roughly the same as the plastic zone shown in Fig. 16g for the same specimen.

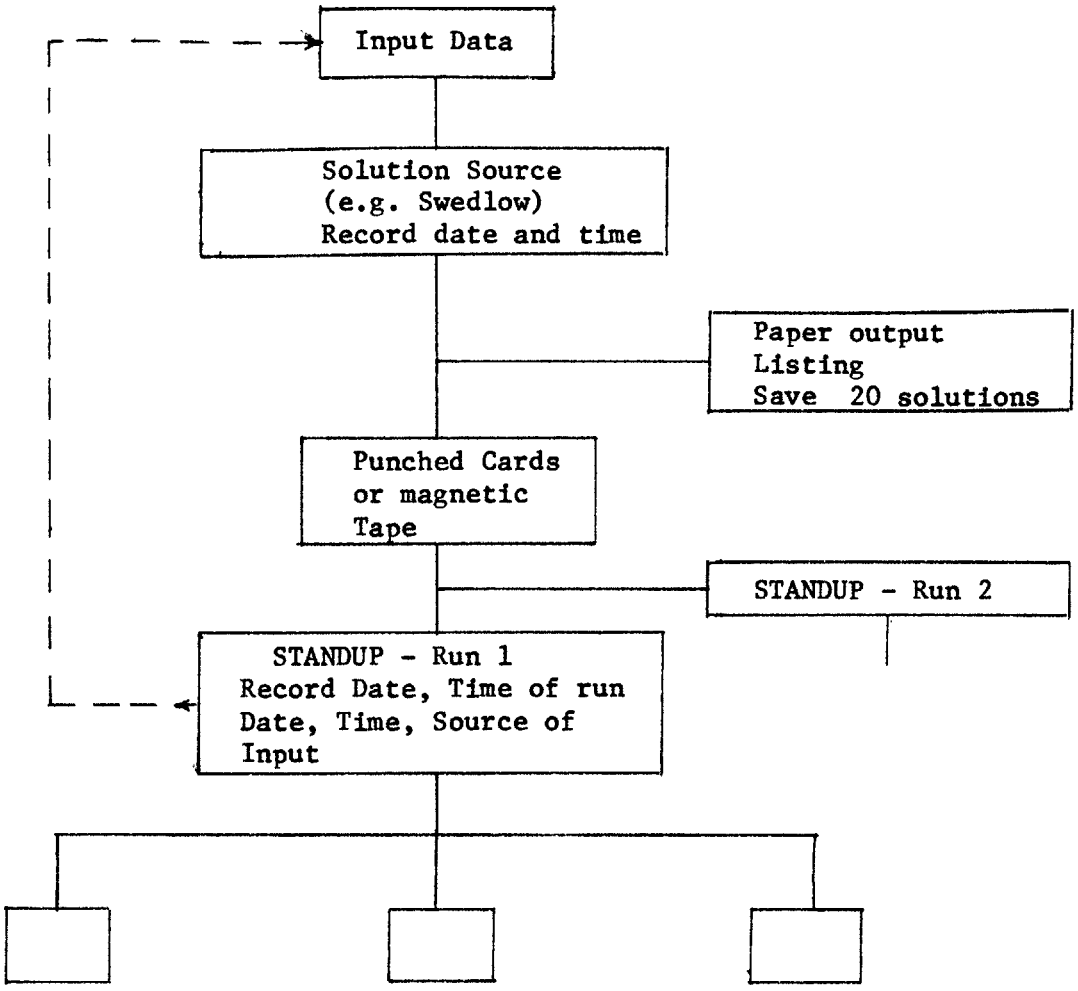

Output Plots - Record Date and
Time of STANDUP

Flow Chart of Programs and Data Sets

Fig. A-1

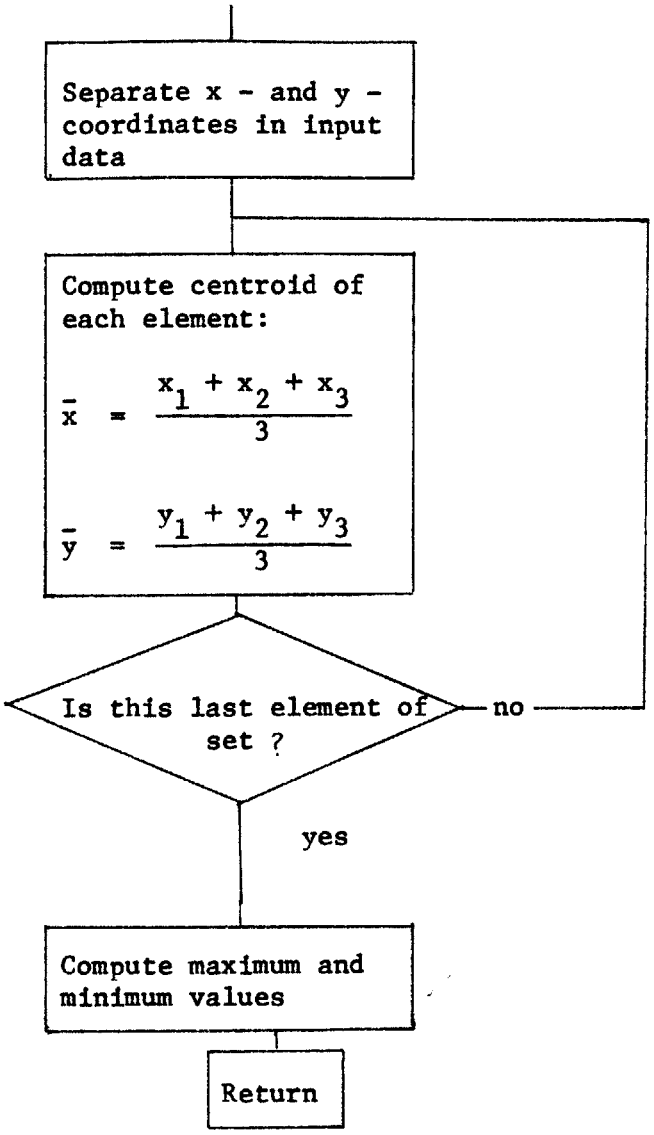

Flow Chart for Subroutine CENTRX

Fig. A-2

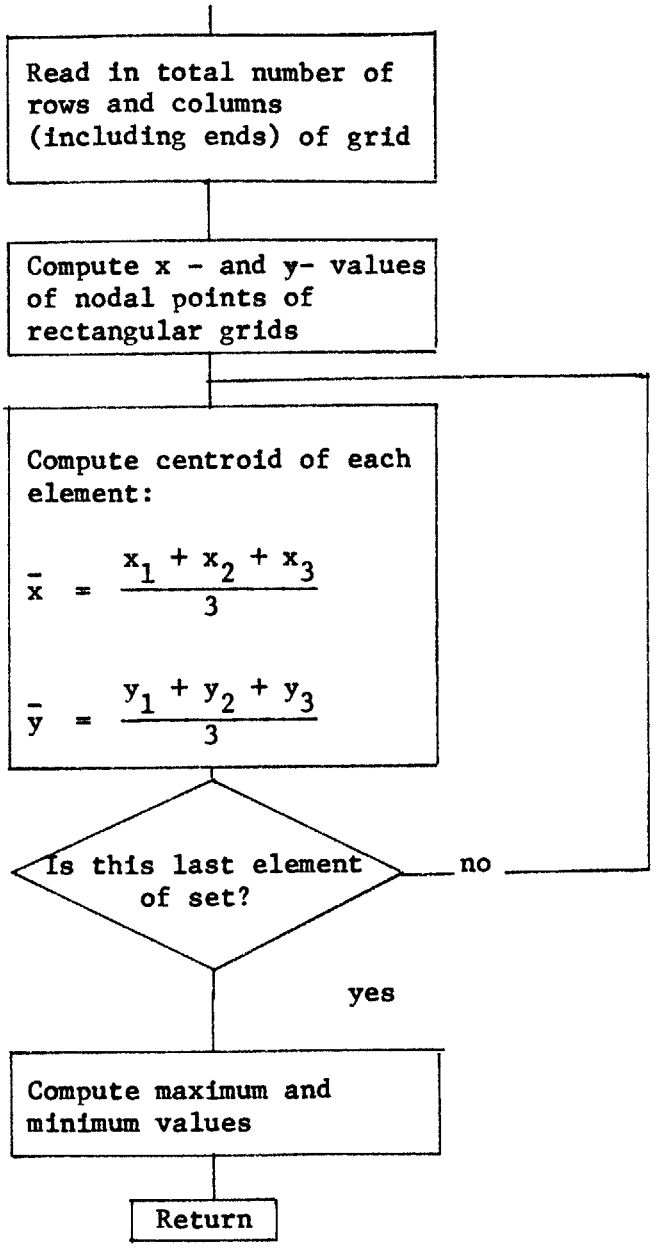

Flow Chart for Subroutine CENTRI

Fig. A-3

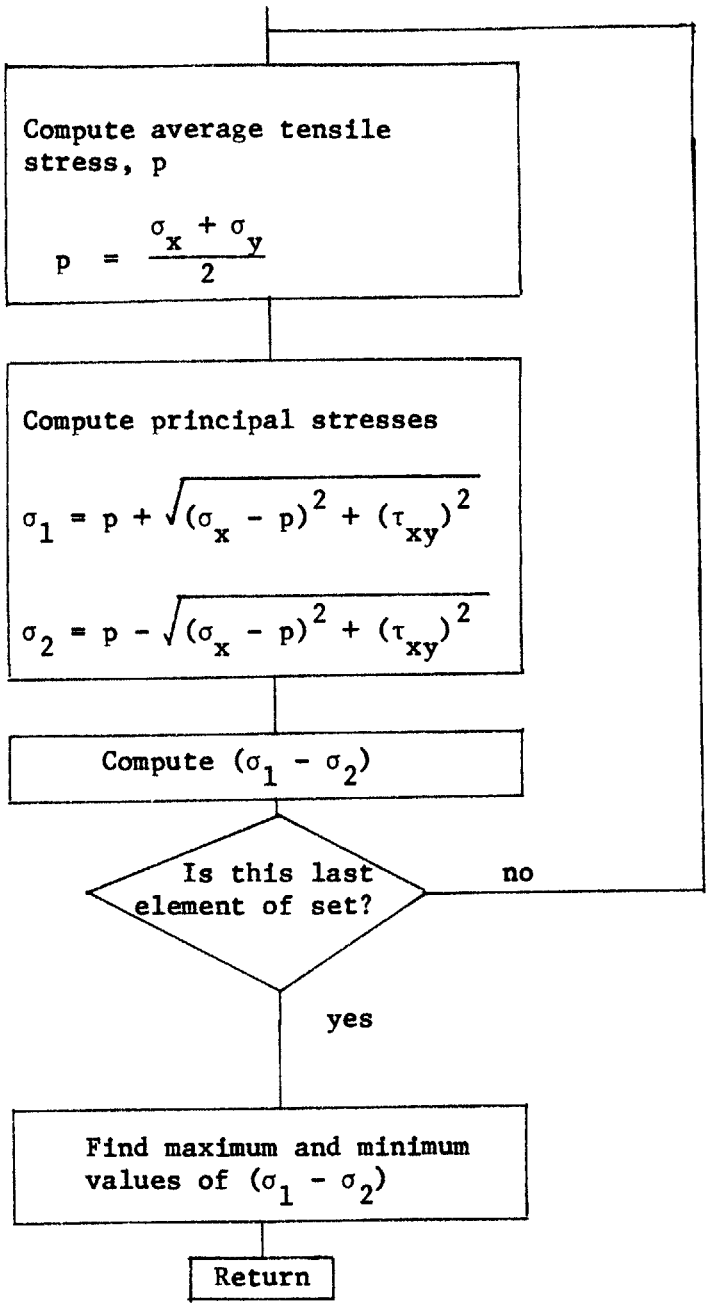

Flow Chart for Subroutine STRESS

Fig. A-4

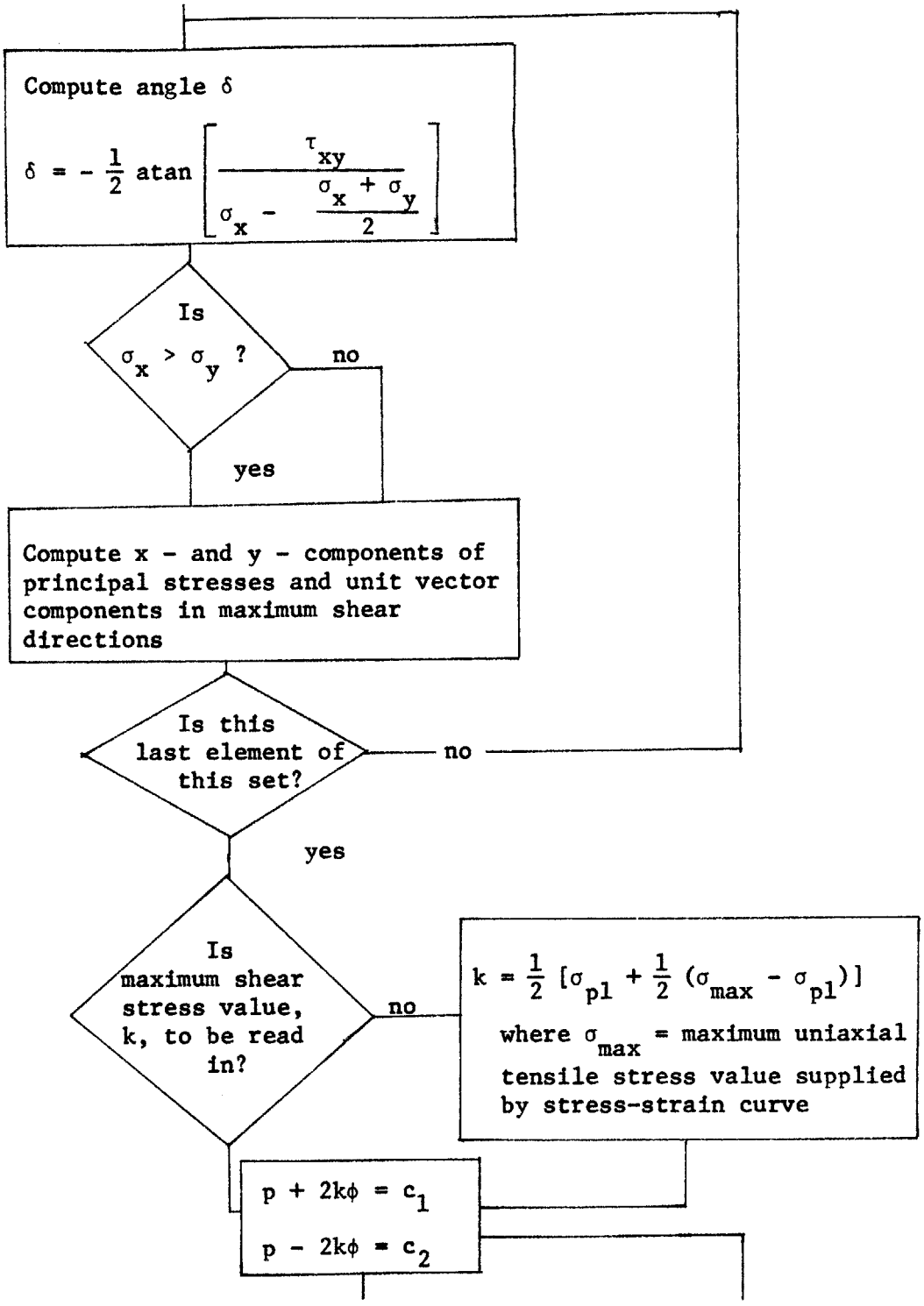

Flow Chart for Subroutine DIRSTS (Direction of Stress)

Fig. A-5

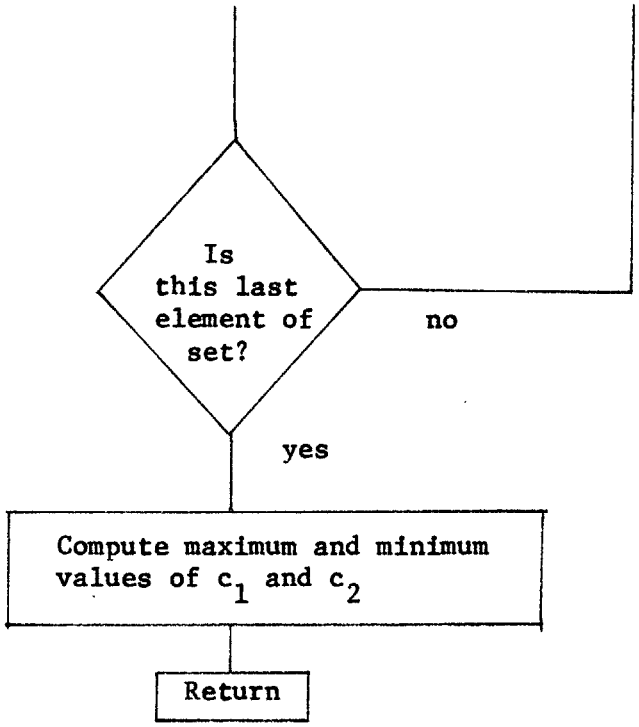
Is this last element of set?
no
yes
Compute maximum and minimum values of c_1 and c_2
Return

Fig. A-5 cont'd

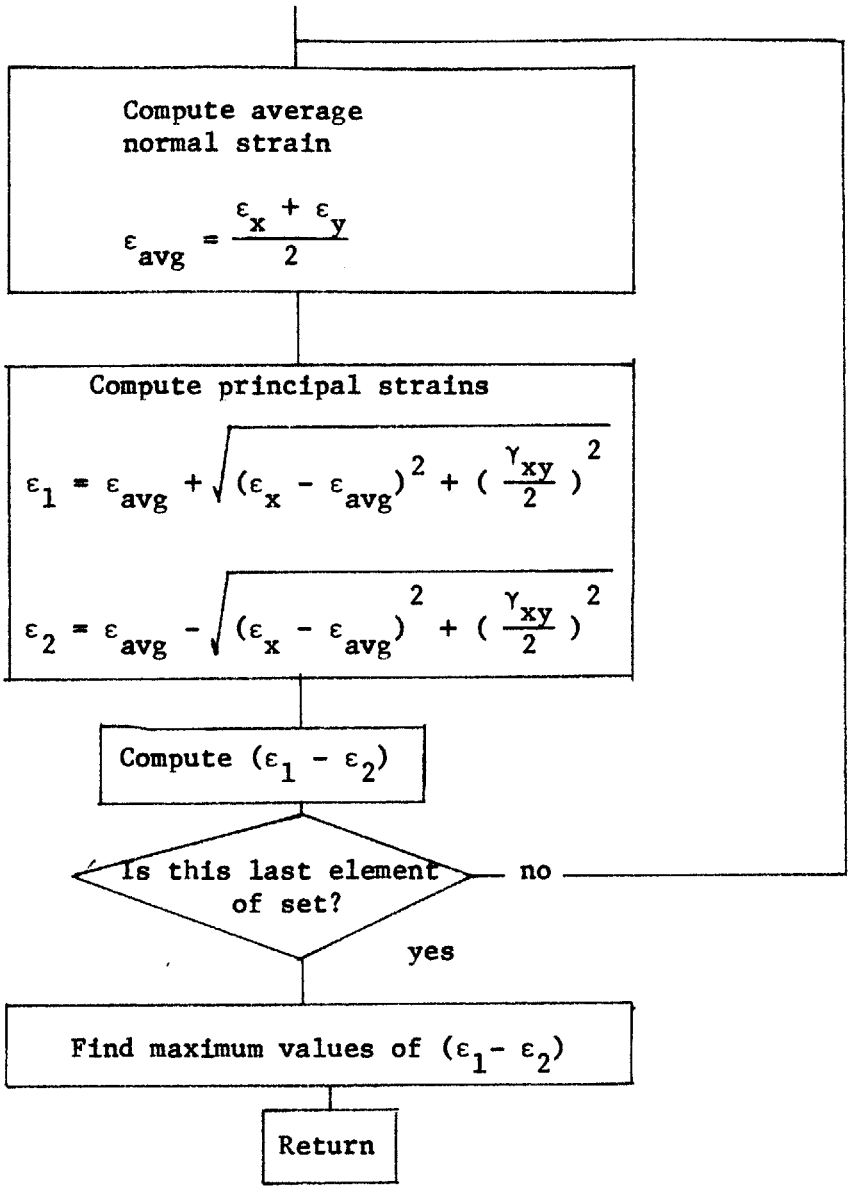

Flow Chart for Subroutine STRAIN

Fig. A-6

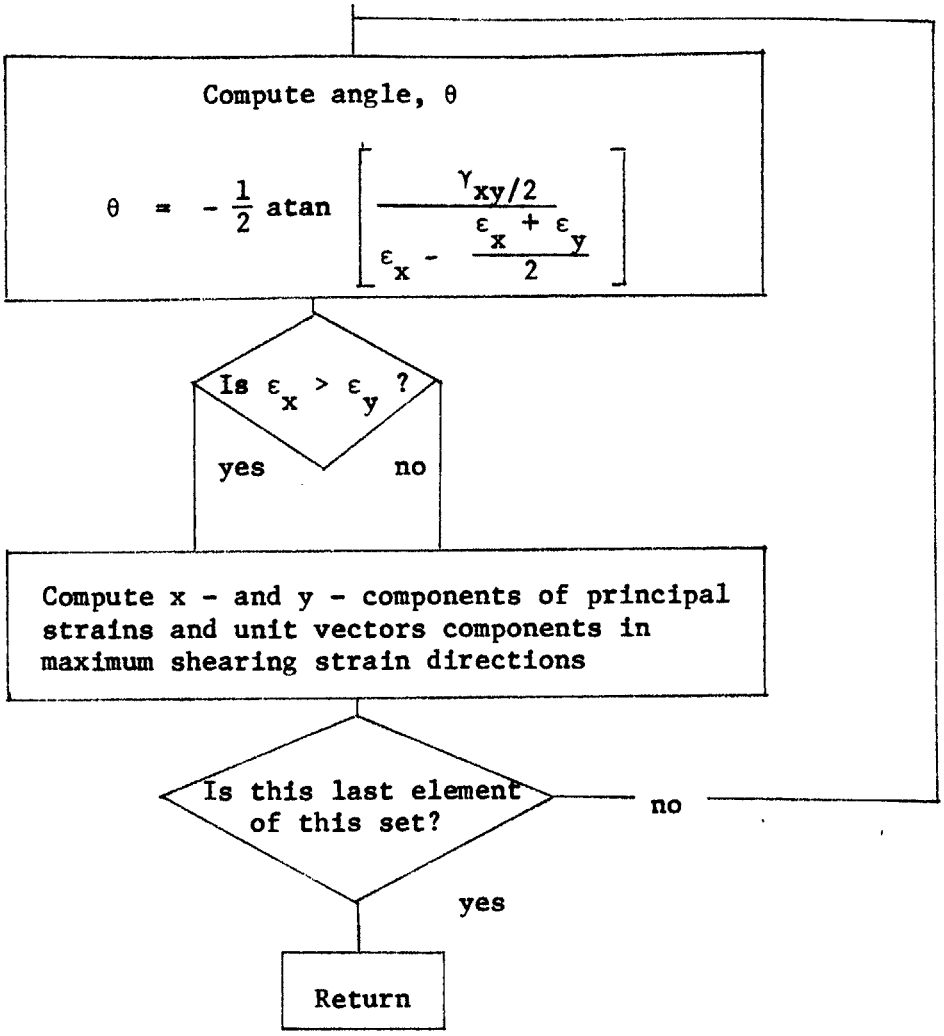

Flow Chart for Subroutine DIRSTN
(Direction of Strain)

Fig. A-7

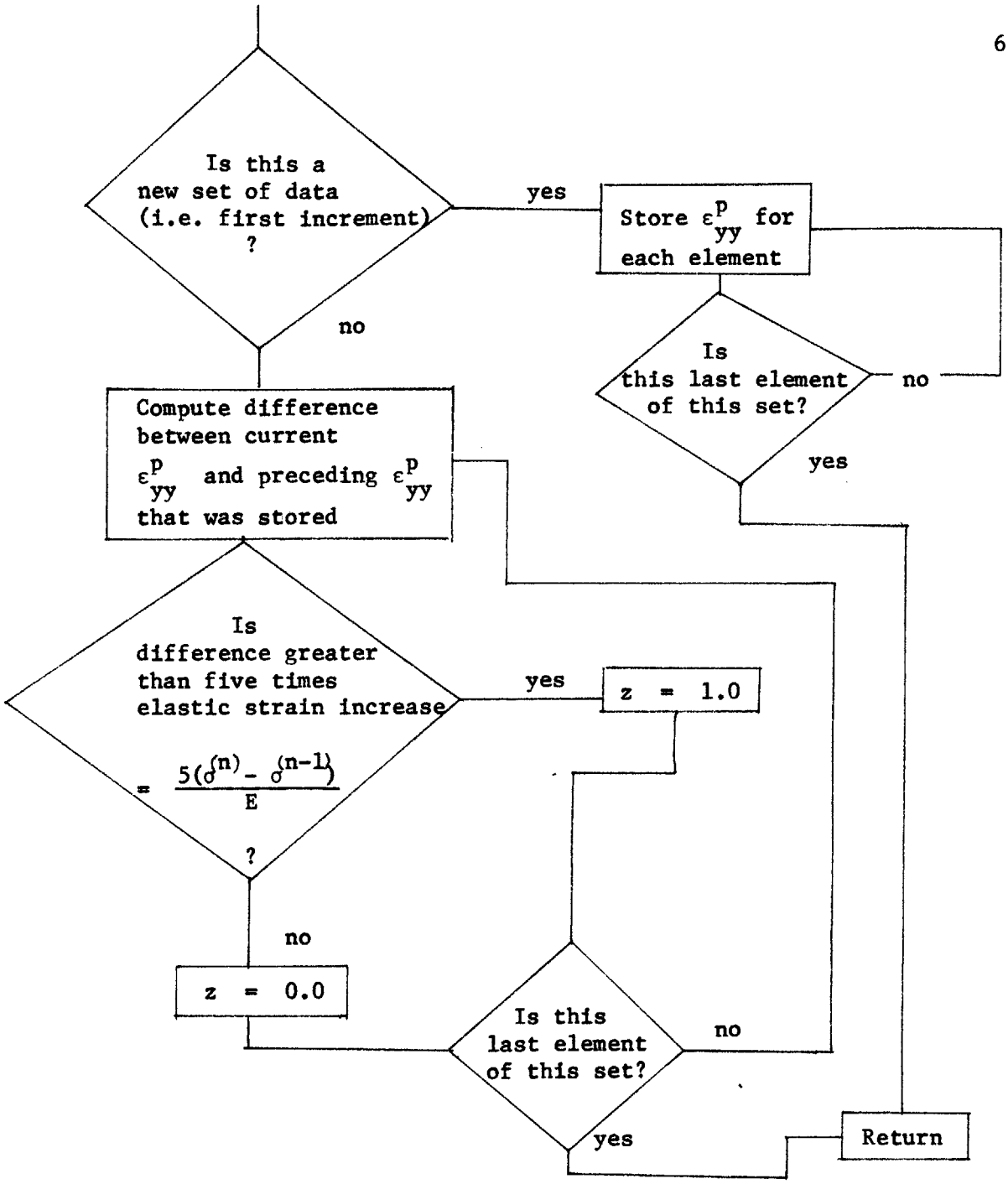

Flow Chart for Subroutine YIELD

Fig. A-8

APPENDIX II

MOTIVATION FOR PUNCHED OUTPUT

Due to the fact that all computer runs of J.L. Swedlow's program had to be made at Carnegie-Mellon University, an attempt was made earlier in the year to get all the output on a magnetic tape for each problem. This was motivated by the voluminous output ($\sim$ 1000 pages per problem). A compatability problem was encountered between the M.I.T. IBM OS/360 and a similar machine at CMU. Once this was overcome, copying each tape became a problem. It also was a very time consuming task (both in man-hours and computer time) to take data from the tape. Early in June it was decided to scrap the tape idea completely and get all the output listing on paper plus certain key information at several load increments on cards. This "key information" consisted of the values that had to be supplied to STANDUP. A total of about ten load increments per problem were chosen to get the punched output. Those chosen always included the first (elastic) for isoclinics, etc. and several sets of succeeding increments for YIELD ZONE. This latter arrangement worked well and since we didn't have to worry about compatability of tapes any more, Swedlow began running his problems on a UNIVAC 1108 with a saving in computer time by a factor of 3 to 1. The air express expense of shipping of about 50 lb of computer listing and

cards has been about $10. It is recommended that the above scheme be followed in any additional problems run on Swedlow's program.

Table I

Review of Numerical Data

Name	Method	Plastic Stress-Strain Law	Strain Hardening	Flow Condition	Axial Boundary	Solutions Reported
Allen and Southwell (1950)	Finite Dif. (Relaxation)	Hencky	No	Mises	$\varepsilon_z^e = \varepsilon_z^p = 0$	Plane stress Plane strain 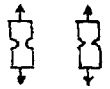
Denke (1956)	Finite Dif.	Ramberg-Osgood	Yes			Simplified swept wing
Wilson (1960)	Linear Increments	Ramberg-Osgood	Yes			Truss, portal frame
Stimpson and Eaton (1961)	Finite Dif. (Relaxation)	Hencky	No	Mises	$\sigma_z = 0$	
Gallagher et. al. (1963)	Finite El.	Incremental (constant stress)	Yes			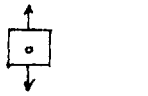
Goldberg and Richard (1963)	Inter-connecting Rods	Ramberg-Osgood	Yes			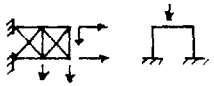
Jurišić (1963)	Finite El.	Prandtl-Reuss	No	Mises	$\varepsilon_z^e = \varepsilon_z^p = 0$	Plane strain (coarse grid) 

Name	Method	Plastic Stress-Strain Law	Strain Hardening	Flow Condition	Axial Boundary	Solutions Reported
Percy et. al (1963)	Finite El.	Hencky	Yes	Mises		Small strain, shear lag
Stricklin (1963)	Finite Dif.		L	Tresca	$\sigma_r = 0$	Thin walled shells of revolution, asymmetric loads, large deflections
Ang and Harper (1964)	Relaxation	Prandtl-Reuss	No	Deformation theory	$\varepsilon_z = 0$ or $\sigma_z = 0$	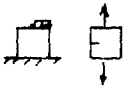
Gallagher et. al. (1964)	Finite El.	$\varepsilon_{ep} = (\frac{\sigma}{\psi})^n$	Yes			Beams, plates, cylinders
Argyris (1965)	Finite El.	Prandtl-Reuss	Yes	Mises		
Lansing et. al. (1965)	Finite El.	Prandtl-Reuss or Hencky	Yes	Mises	$\sigma_z = 0$	Shear lag

Name	Method	Plastic Stress-Strain Law	Strain Hardening	Flow Condition	Axial Boundary	Solutions Reported
Pope (1965)	Finite El.	Incremental	L	Mises	$\sigma_z = 0$ or $\epsilon_z = 0$	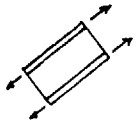
Swedlow et. al. (1965)	Finite El.	Prandtl-Reuss	Yes	Mises	$\epsilon_z = 0$ or $\sigma_z = 0$	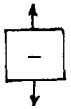
Booy (1966)	Finite Dif. (non-iterative)					Slow viscous flow in long tube
Mentel (1966)	Finite El.	Ramberg-Osgood	Yes	Deformation theory		Truss
Parmalee (1966)	Finite El.	Elastic only				 2-D and 3-D 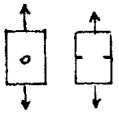
Fowler (1967)	Finite El.	Hencky	Yes	Mises	$\sigma_r = 0$	Thin walled shells of revolution, asymmetric loads (small deflections)

Name	Method	Plastic Stress-Strain Law	Strain Hardening	Flow Condition	Axial Boundary	Solutions Reported
Isakson et. al. (1967)	Finite El.	Ramberg-Osgood	Yes	Mises	$\sigma_z = 0$	Notched bar stiffened panel
Wilson and Jones (1967)	Finite El.	Elastic only				
Speare (1968)	Finite El.	Elastic only				Small deflections
Butler (1969)	Finite El.	Elastic only				2-D and 3-D

Table II.

Notched Tensile Problem Parameters

Included Angle, ω	52°	0°
Net half section, a	0.07	0.10
Radius, r	0.02	0.02
Half width, w	0.50	0.53
Half length, ℓ	1.10	0.80
Plastic constraint factor, f	1.85	2.11
Number of elements	342	400
Number of nodes	200	231
Number of stress load increments	34	38
Min. applied stress on net section normalized with respect to uniaxial tensile strength	0.43	0.26
Max. applied stress on net section	2.79	3.28
Stress-strain curve	Fig. 1	Fig. 2
1108 Computation time (minutes)	7	10
Computation cost	$50	$75

Table III. Input Data to Isochromatics

```
OF CING D ZOLINEHROMLINIAIN ESS I   TAPEINPUDATASTOPU=0 V=0          DATA CARD 1
INPUT DATA
PLATE W/CENTER HOLE - BIAXIAL COMPRESSION + TENSION.SWEDLOW RUN 7-26-68
 28 242 200  22  31          40
              .33333           10800000.
                    .00000000          23570.215        1          DATA1036
                    .00005500          24041.621        2          DATA1037
                       :                  :
                    14.13100290        80138.687        30         DATA1065
                    45.94885300        94280.813        31         DATA1066
 12  21  34  43  56  65  78  87 100 109 122 131 144 153 166 175 188 197
210 219 232 241
  16000.    500.    500.    500.    500.    500.    500.    500.    500.DATA1002
   1000.   1000.   1000.   1000.   1000.   1000.   1000.   1000.   1000.DATA1003
   1000.   1000.   1000.   1000.   1000.   1000.   1000.   1000.   1000.DATA1004
   1000.   1000.   1000.   1000.   1000.   1000.   1000.   1000.   1000.DATA1005
   1000.   1000.   1000.   1000.                                        DATA1006
  1 12  2   2 14  3   3 14  4   4 16  5   5 16  6   1  7 12   7  8 19  DATA1007
  8  9 19   9 10 21  10 11 21   2 12 13   2 13 14   4 14 15   4 15 16  DATA1008
                       :                                  :
109110120 101111112 101112113 103113114 103114115 105115116 106117111  DATA1034
106118117 108119118 108120119 110121120                                DATA1035
  0.99999934  0.99999875                                               66
  0.99999928  0.72654158                                               55
      :           :
  0.01564367  0.09876877                                              100
  0.00000032  0.09999996                                              111
START OF COMMANDS
ISOCHROMATIC STRESS
DATA
  1   1
  1
    16000.          32.24549            .00000          32.24549      1000
  1.9375 -1.9375 1.0019  .9981  1.337 -1.335  -.002  1.00 -1.00  -.00  .00 1001
  1.9804 -1.3967 1.0020  .7251  1.330 -1.328  -.030  1.00  -.99  -.01  .00 1002
                    :                                  :
   .0756  -.5168  .0157  .0983  1.225 -1.027   .181  1.07  -.62   .07  .15 1120
   .0000  -.5153  .0000  .0995  1.663 -1.619  -.044  1.28 -1.18  -.02  .03 1121
  1.37896 -1.60178 -.54589  .86711 -1.36845 -.20471 -.16712          1122
  1.32879 -1.45941 -.51997  .89863 -1.19252 -.19499 -.09796          1123
                    :                                  :
  2.91763 -1.27776 -1.35305  3.41813  .27158 -.50739  1.22990        1199
  3.26284 -1.57992  -.19043  3.70931  .07725 -.07141  1.26219        1200
STOP
END OF COMMANDS
```

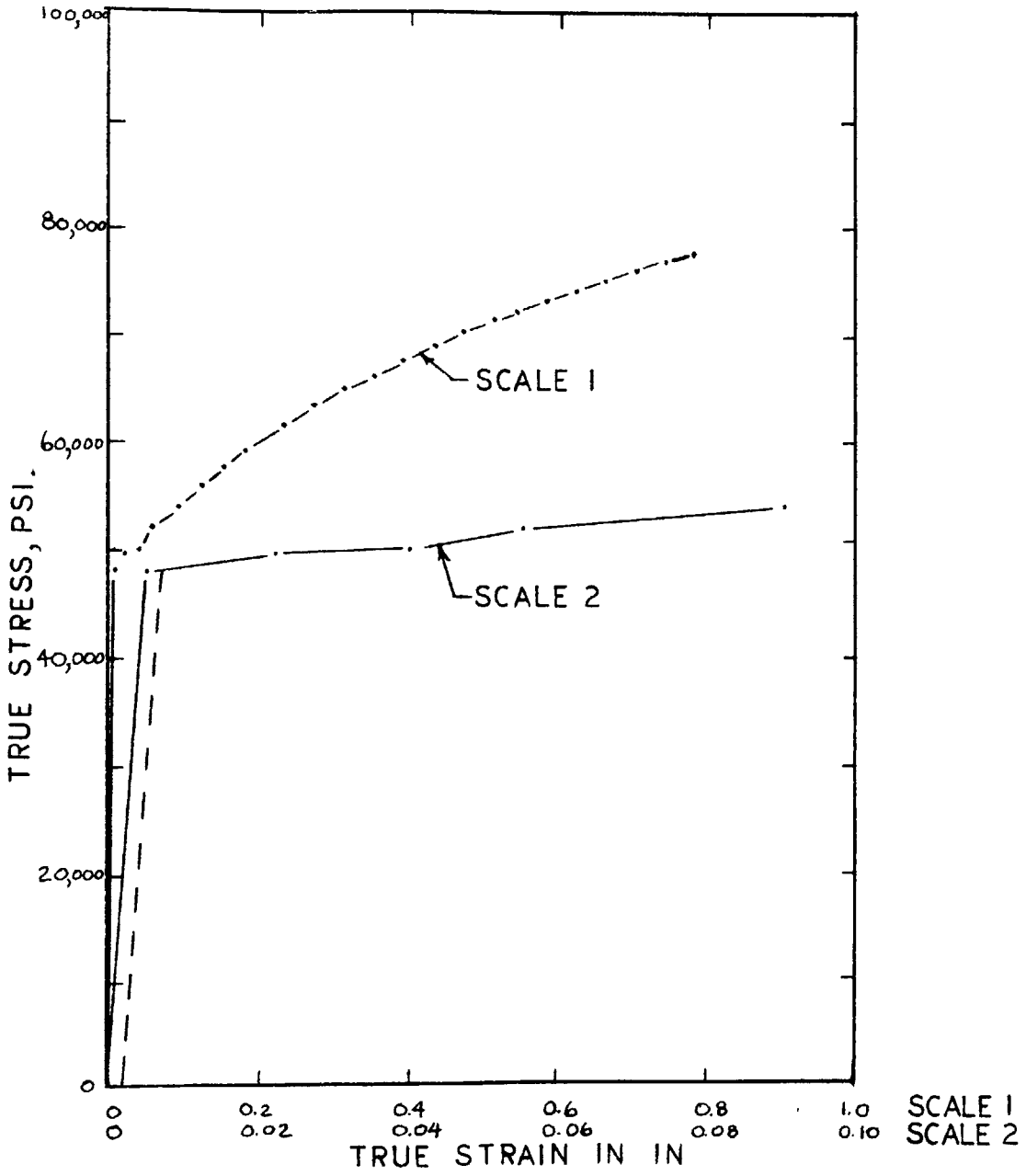

STRESS-STRAIN CURVE 1
6061-T6 ALUMINUM
FIG. 1

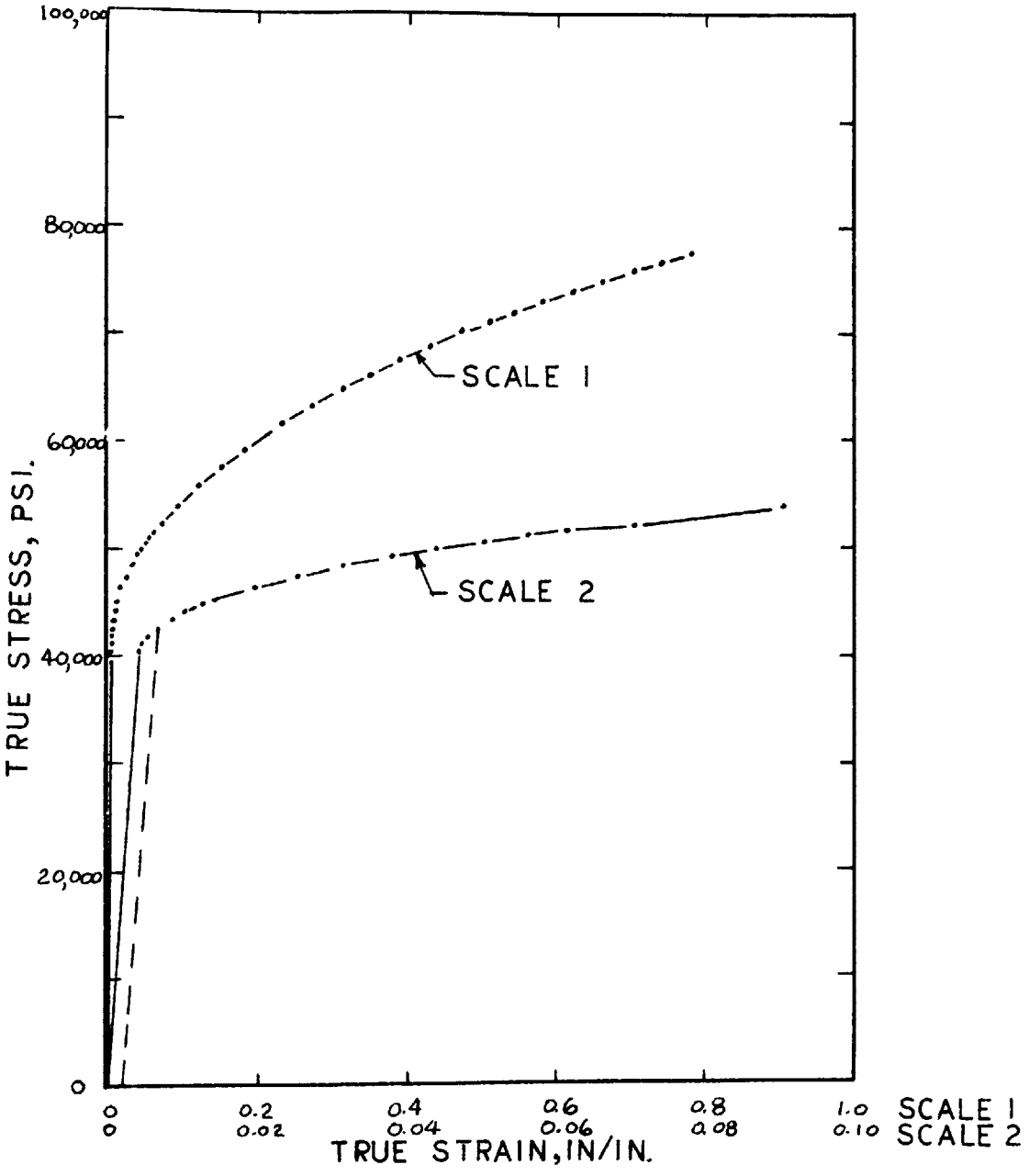

STRESS-STRAIN CURVE 2
6061-T6 ALUMINUM
FIG. 2

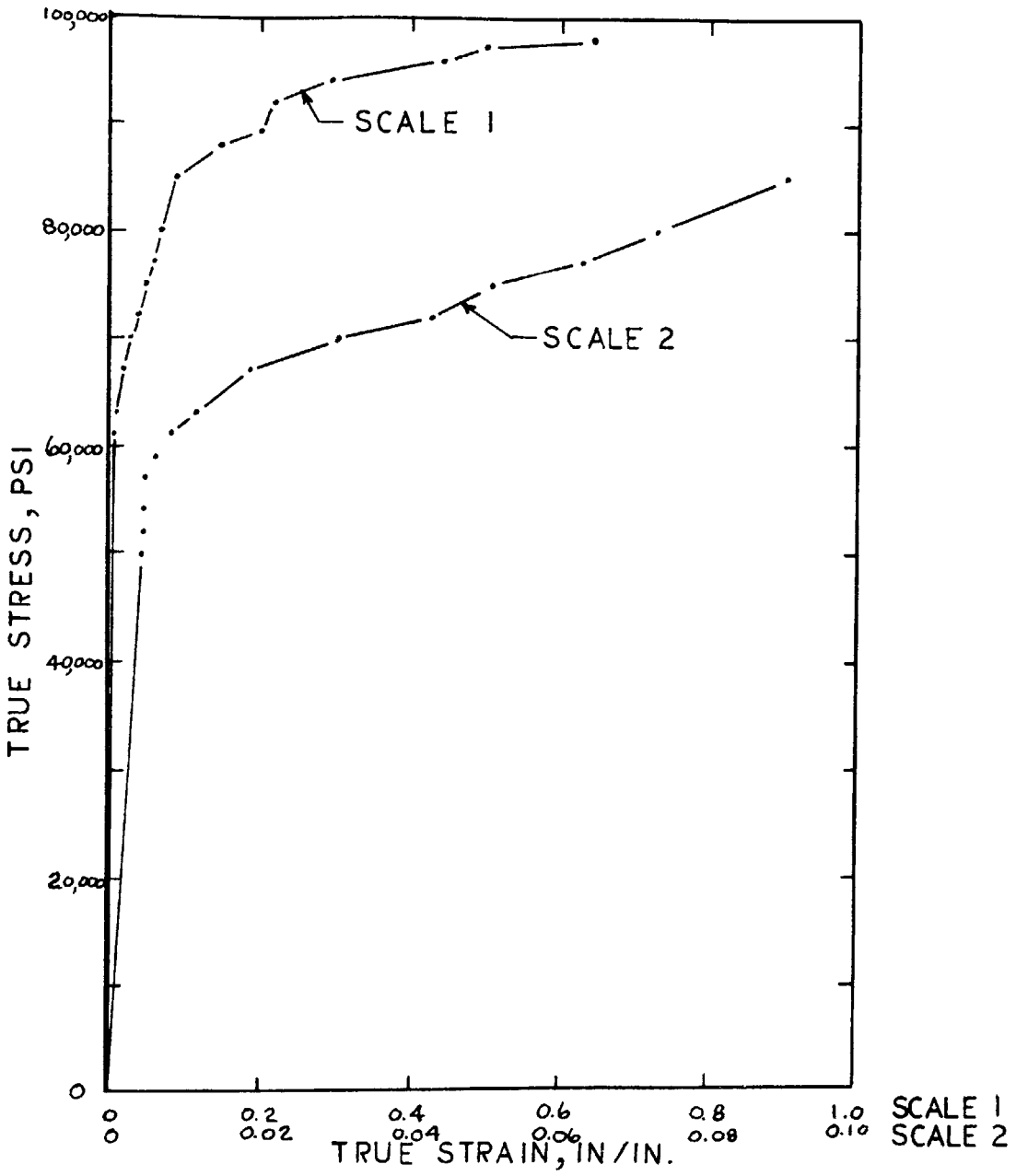

STRESS-STRAIN CURVE
2024-T4 ALUMINUM
FIG. 3

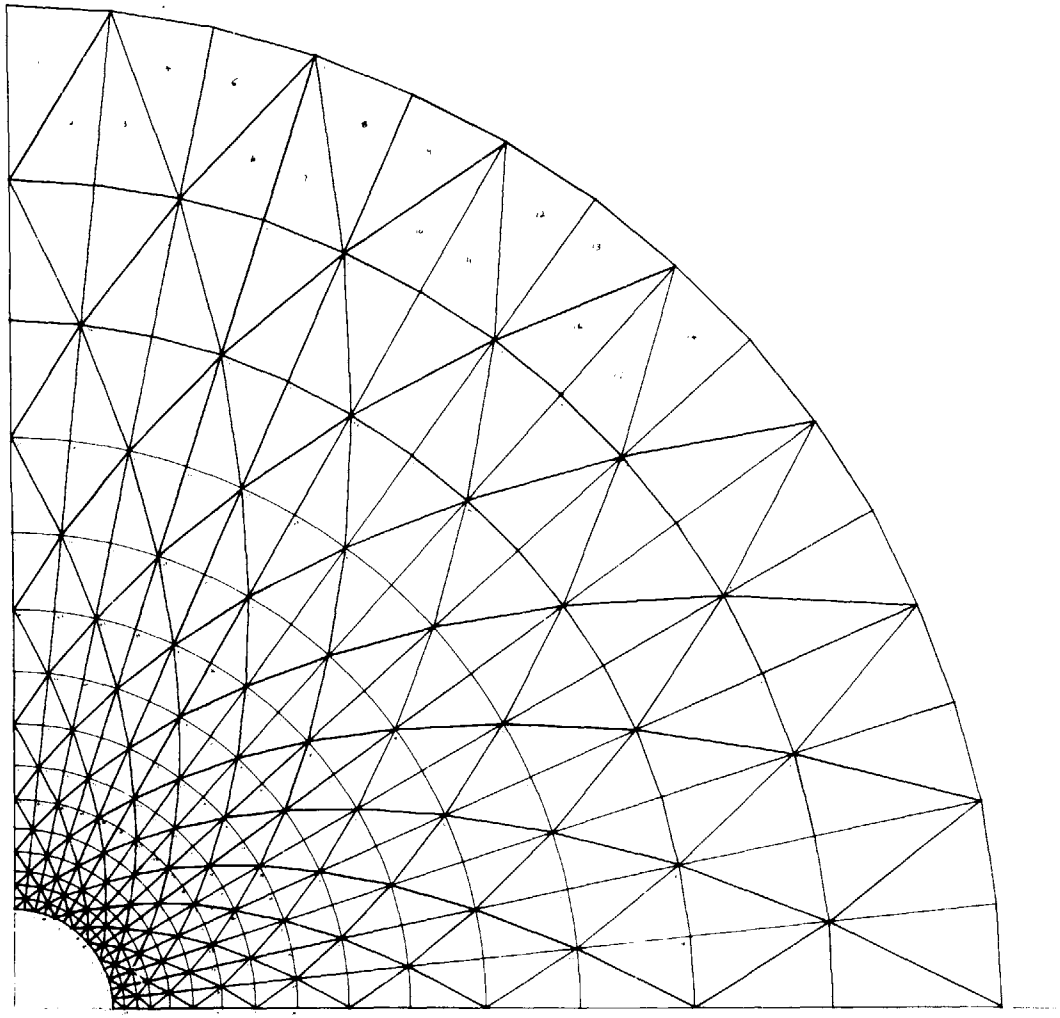

THICK-WALLED CYLINDER QUADRANT
FIG. 4

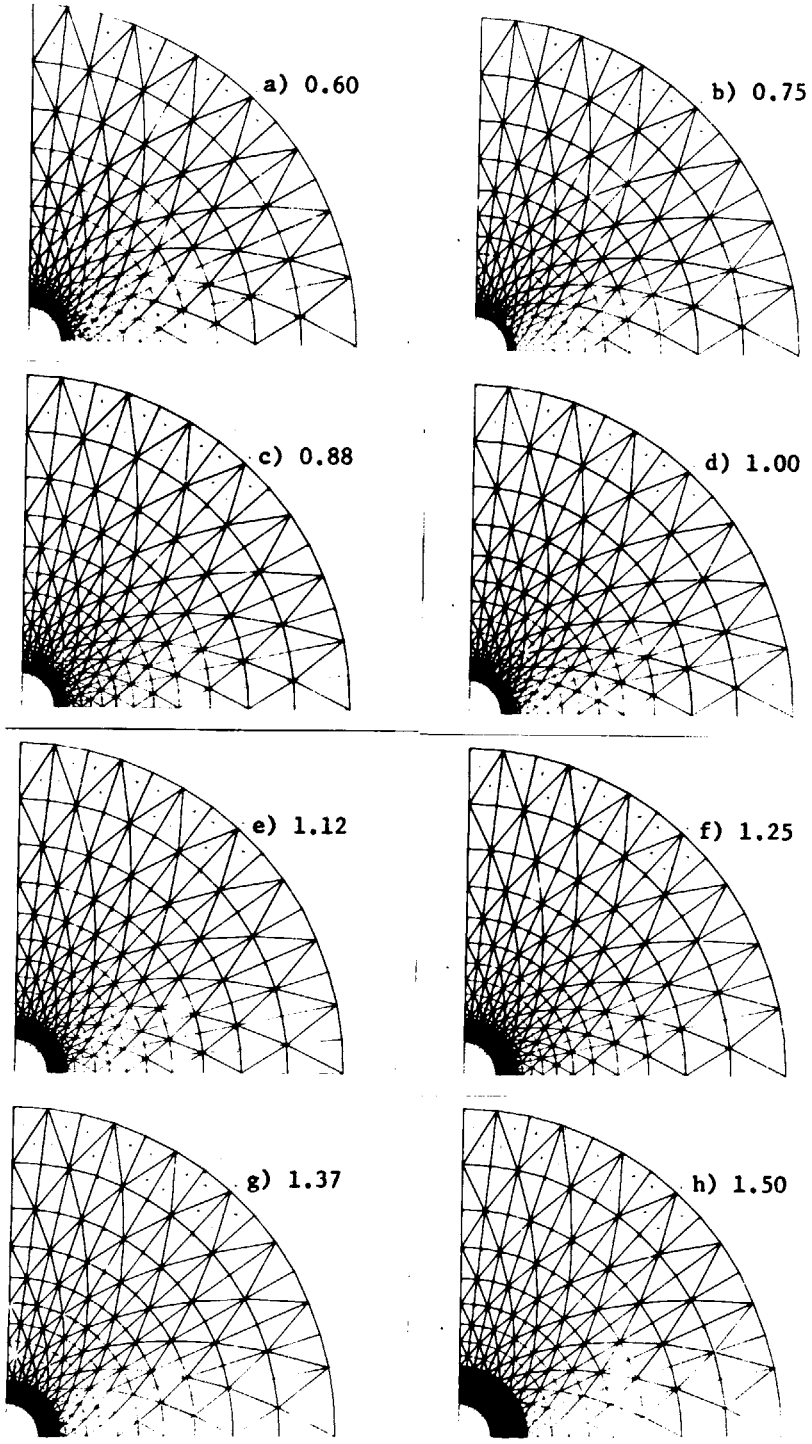

GROWTH OF PLASTIC ZONE IN THICK-WALLED CYLINDER, FIG. 5

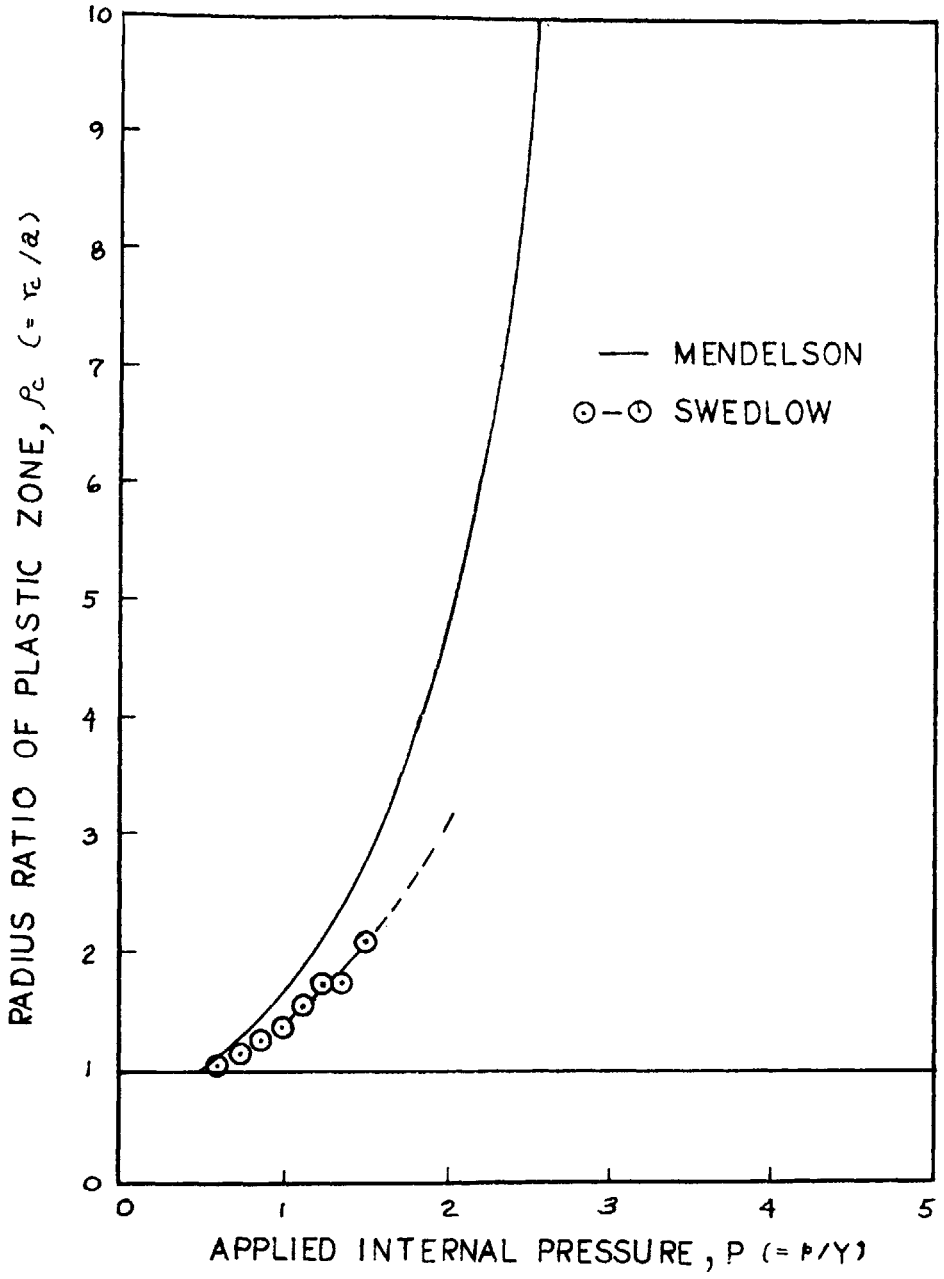

RADIUS OF PLASTIC ZONE
vs. APPLIED INTERNAL PRESSURE
THICK-WALLED CYLINDER

FIG. 6

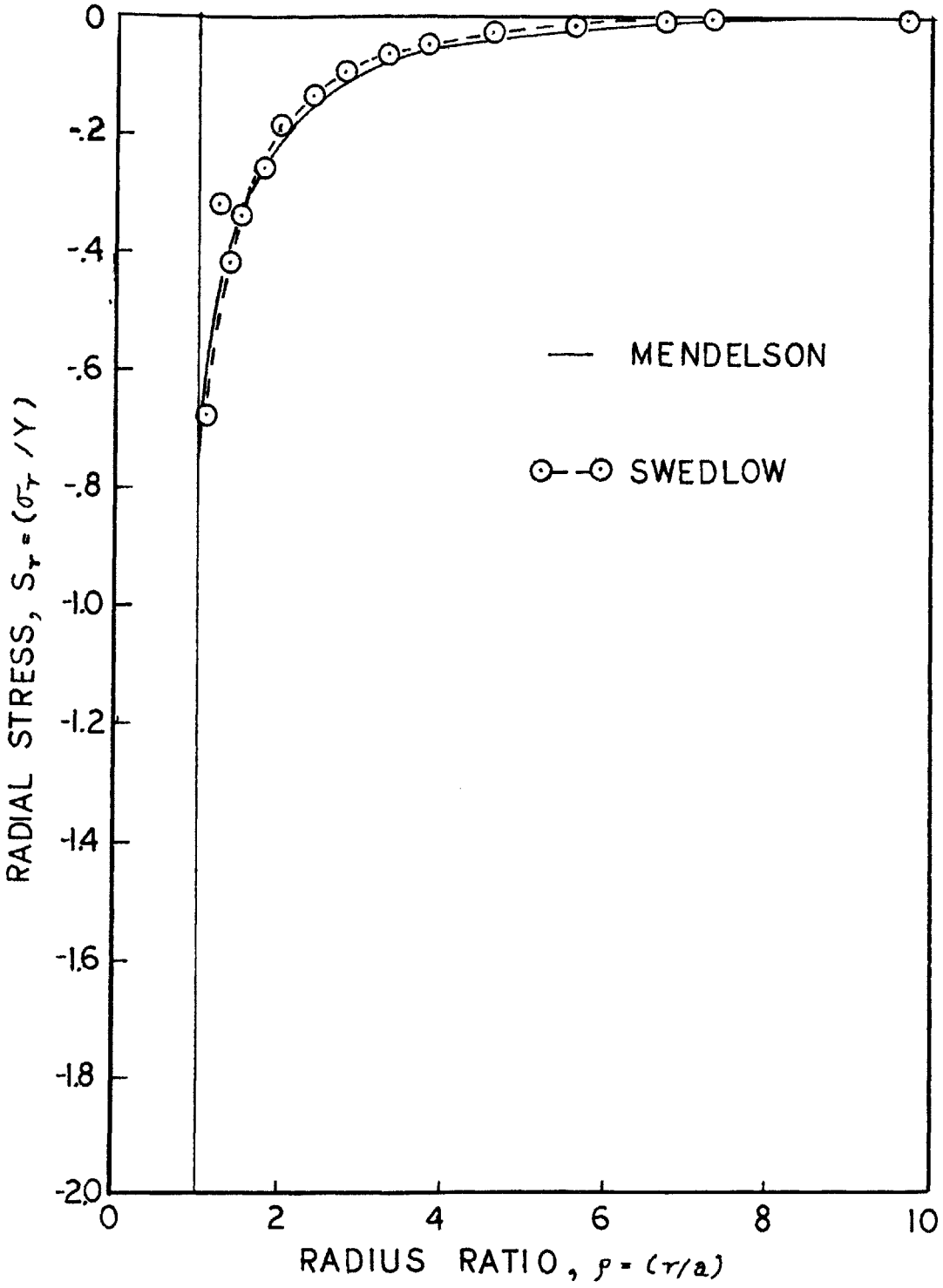

RADIAL STRESS vs RADIUS RATIO
THICK-WALLED CYLINDER, P=0.75
FIG. 7

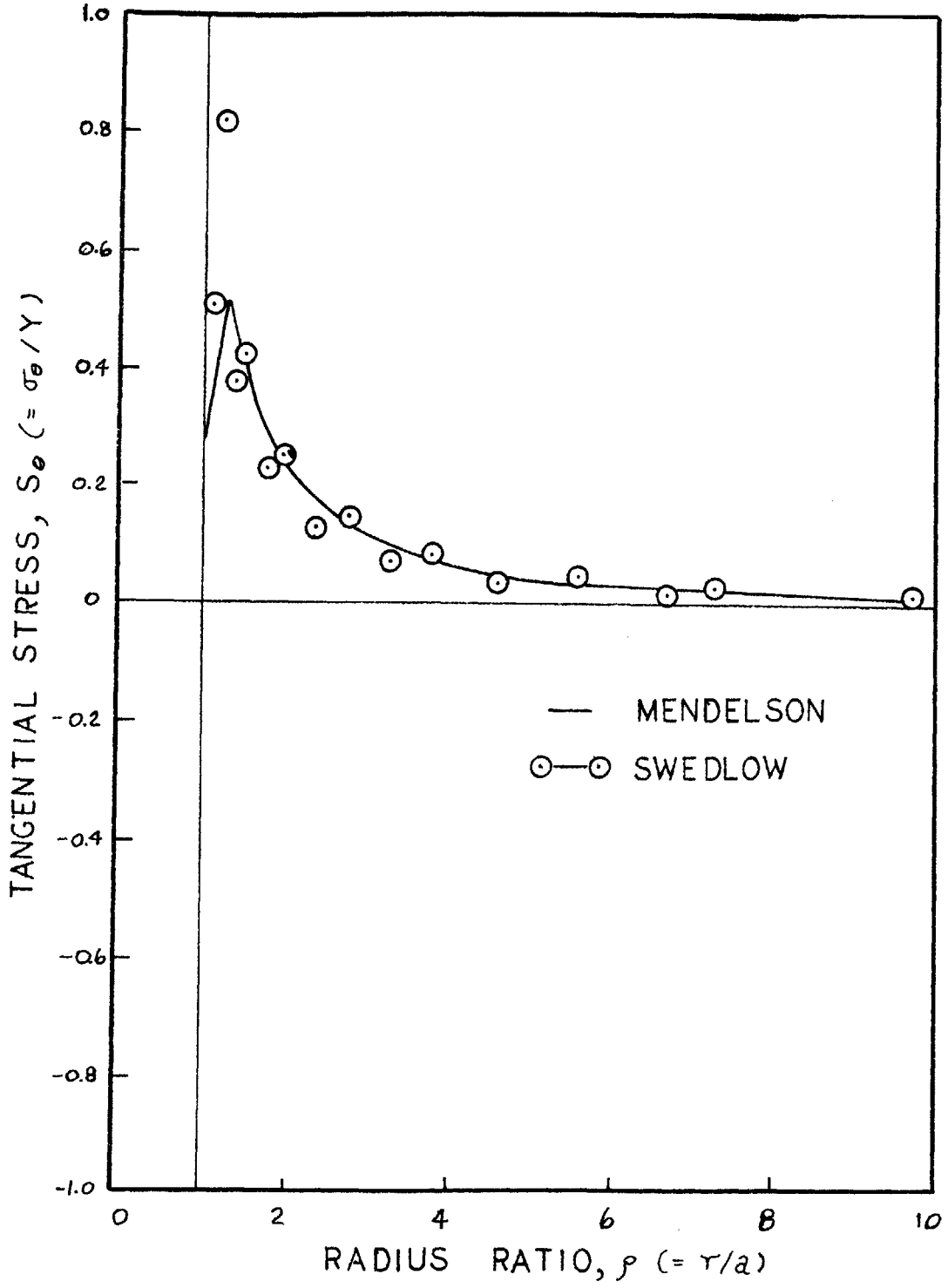

TANGENTIAL STRESS vs. RADIUS RATIO
THICK-WALLED CYLINDER, P=0.75

FIG. 8

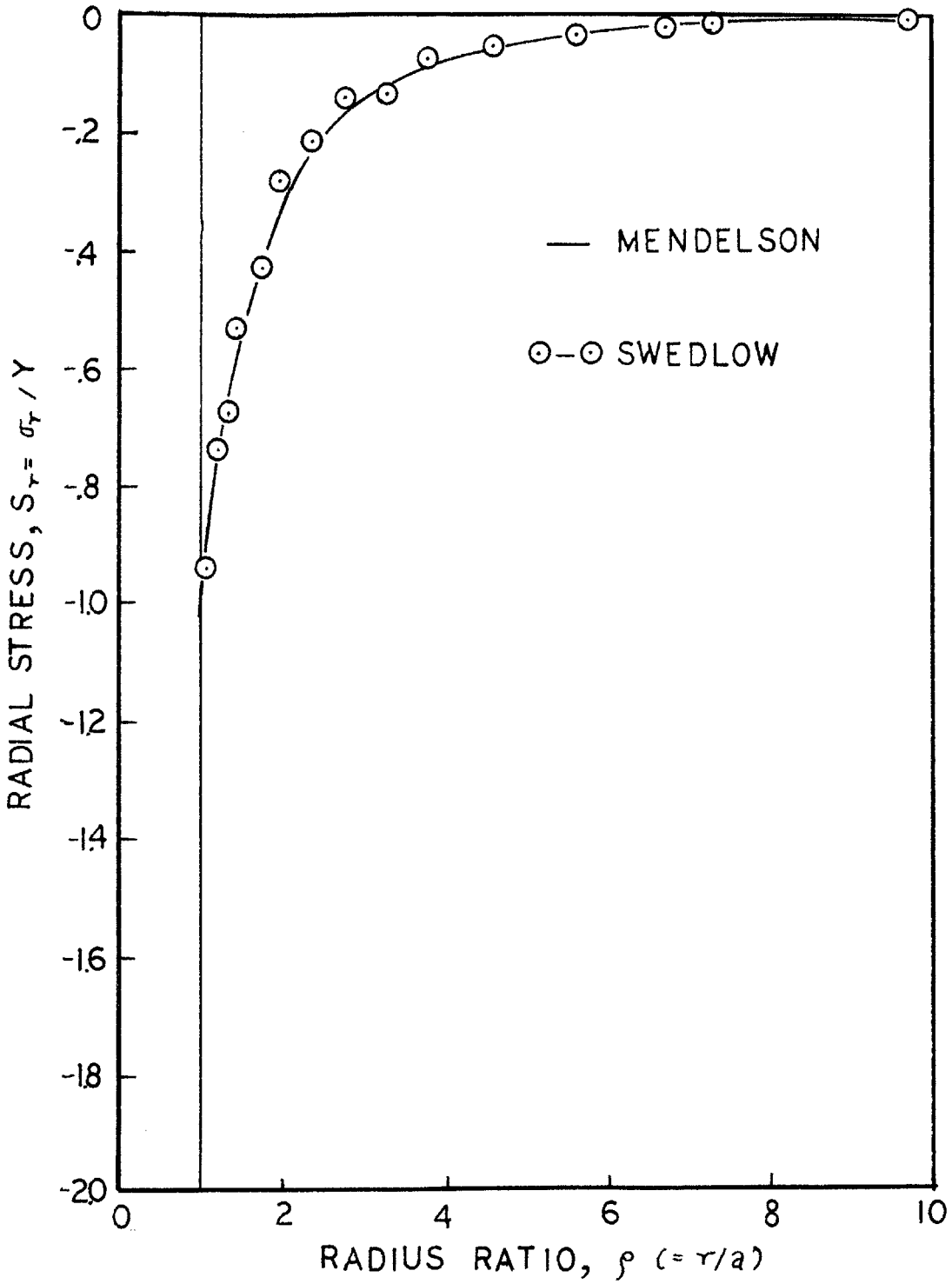

RADIAL STRESS vs. RADIUS RATIO
THICK-WALLED CYLINDER, P = 1.0

FIG. 9

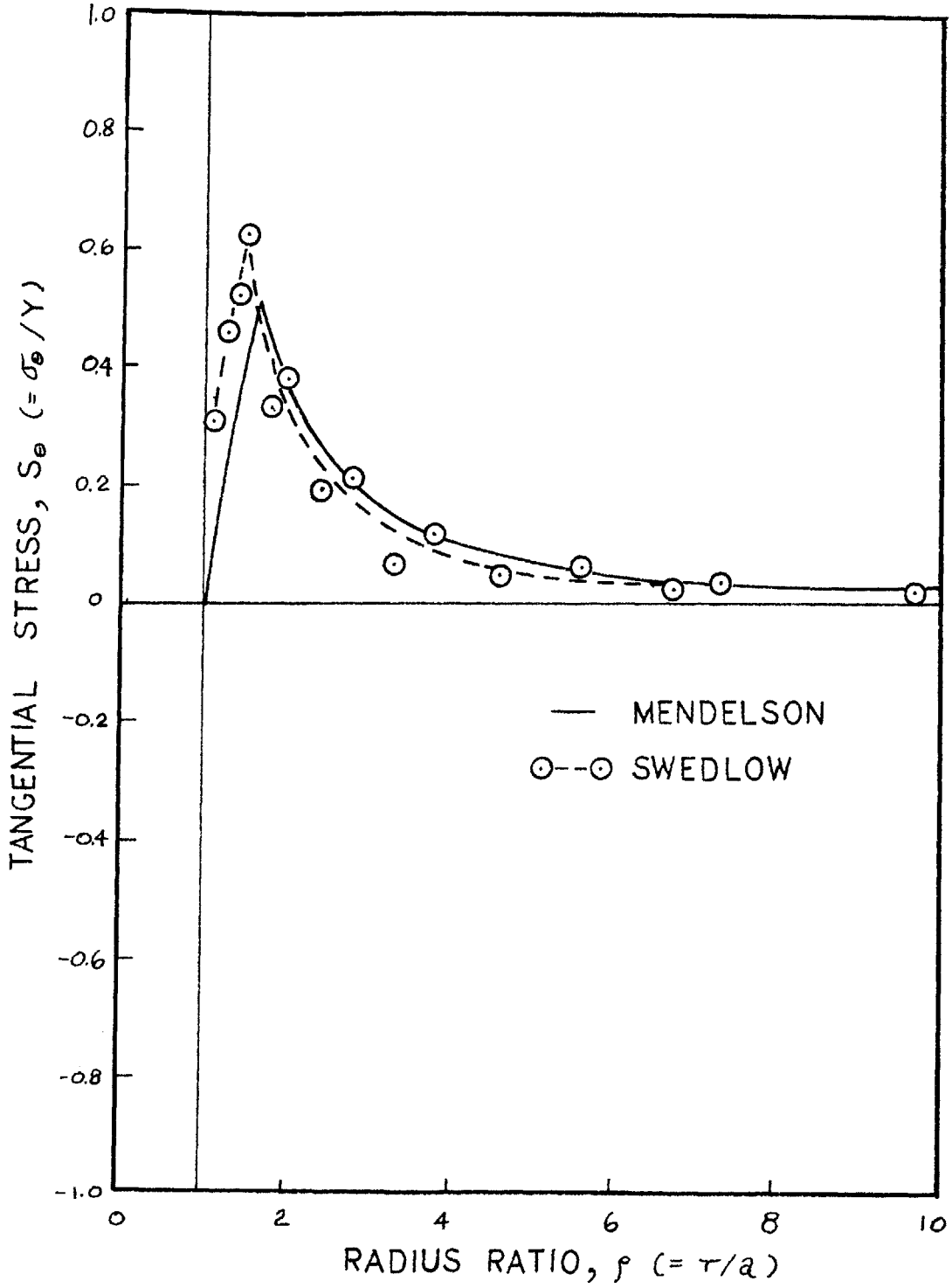

TANGENTIAL STRESS vs. RADIUS RATIO
THICK-WALLED CYLINDER, P = 1.0

FIG. 10

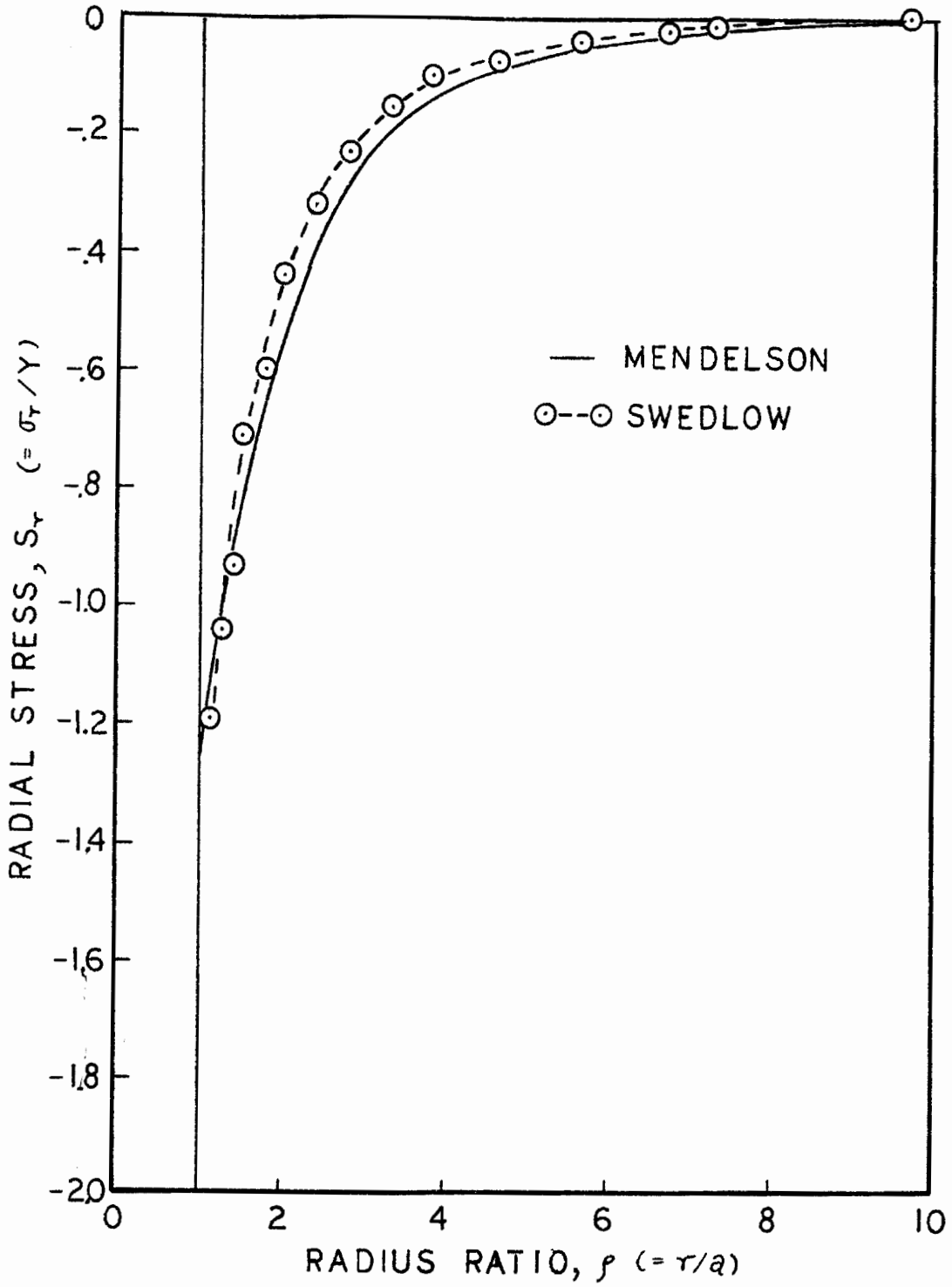

RADIAL STRESS vs. RADIUS RATIO
THICK-WALLED CYLINDER, P = 1.25

FIG. 11

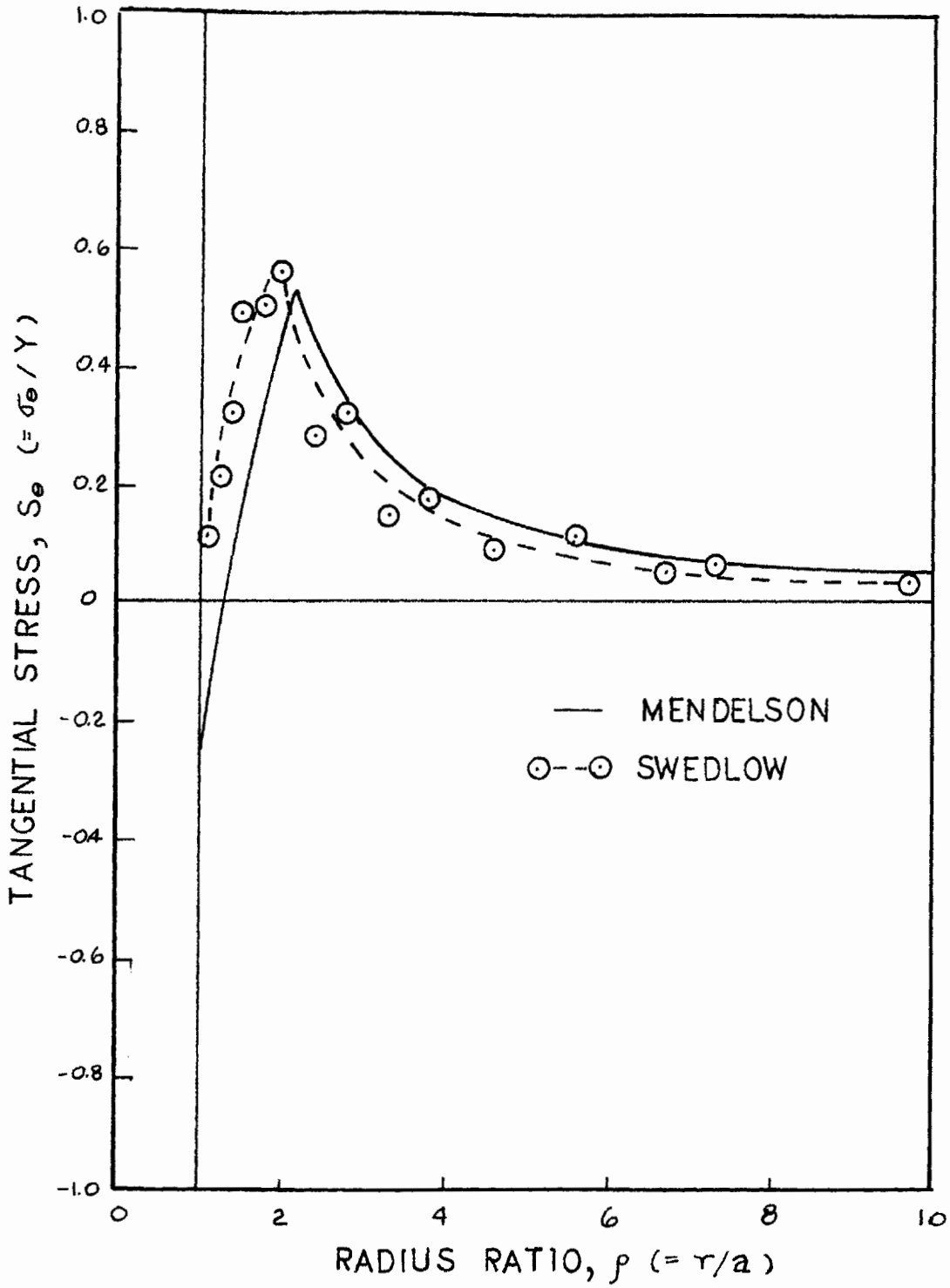

TANGENTIAL STRESS vs. RADIUS RATIO
THICK-WALLED CYLINDER, P=1.25

FIG. 12

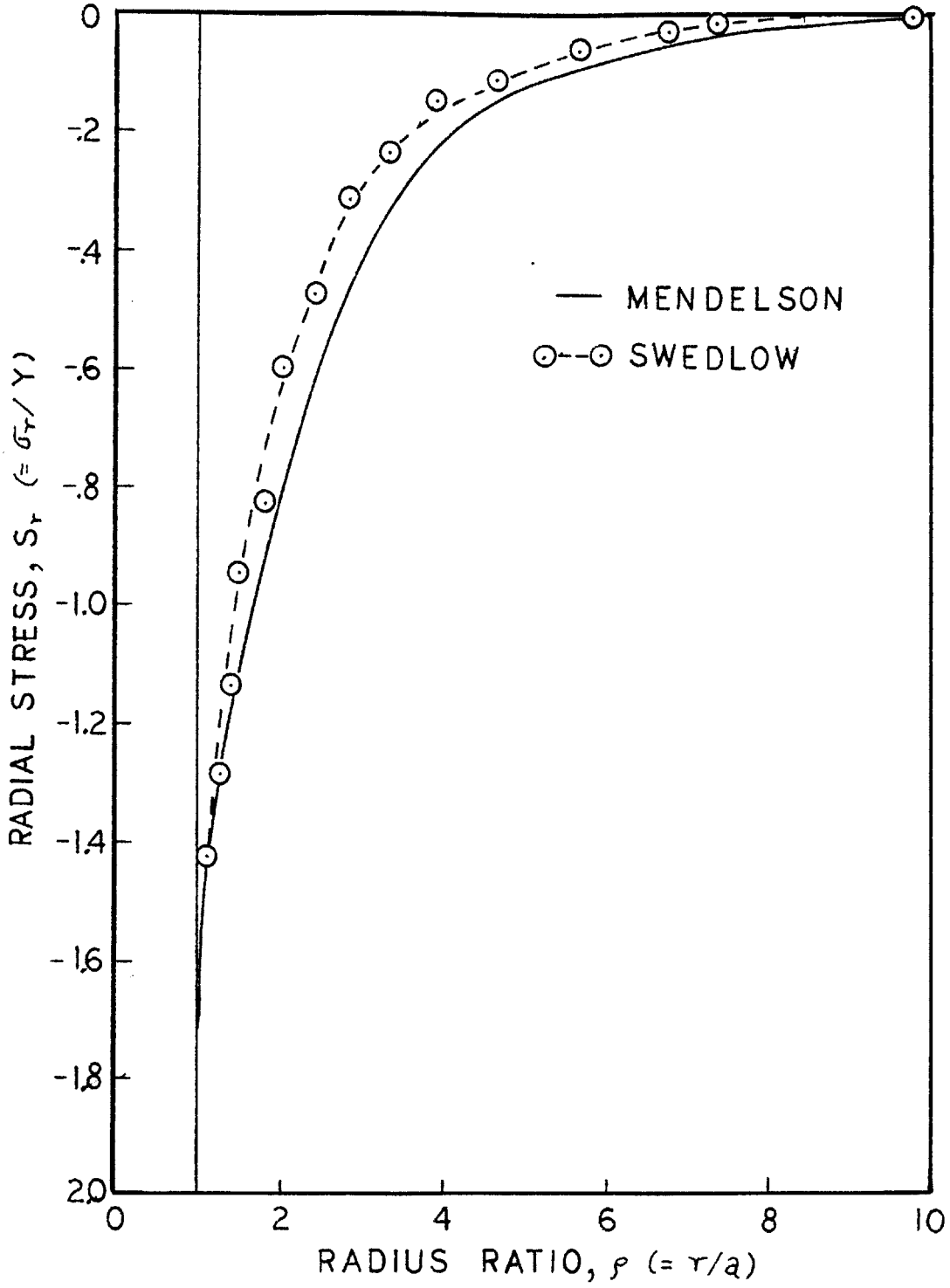

RADIAL STRESS vs. RADIUS RATIO
THICK-WALLED CYLINDER, P = 1.50

FIG. 13

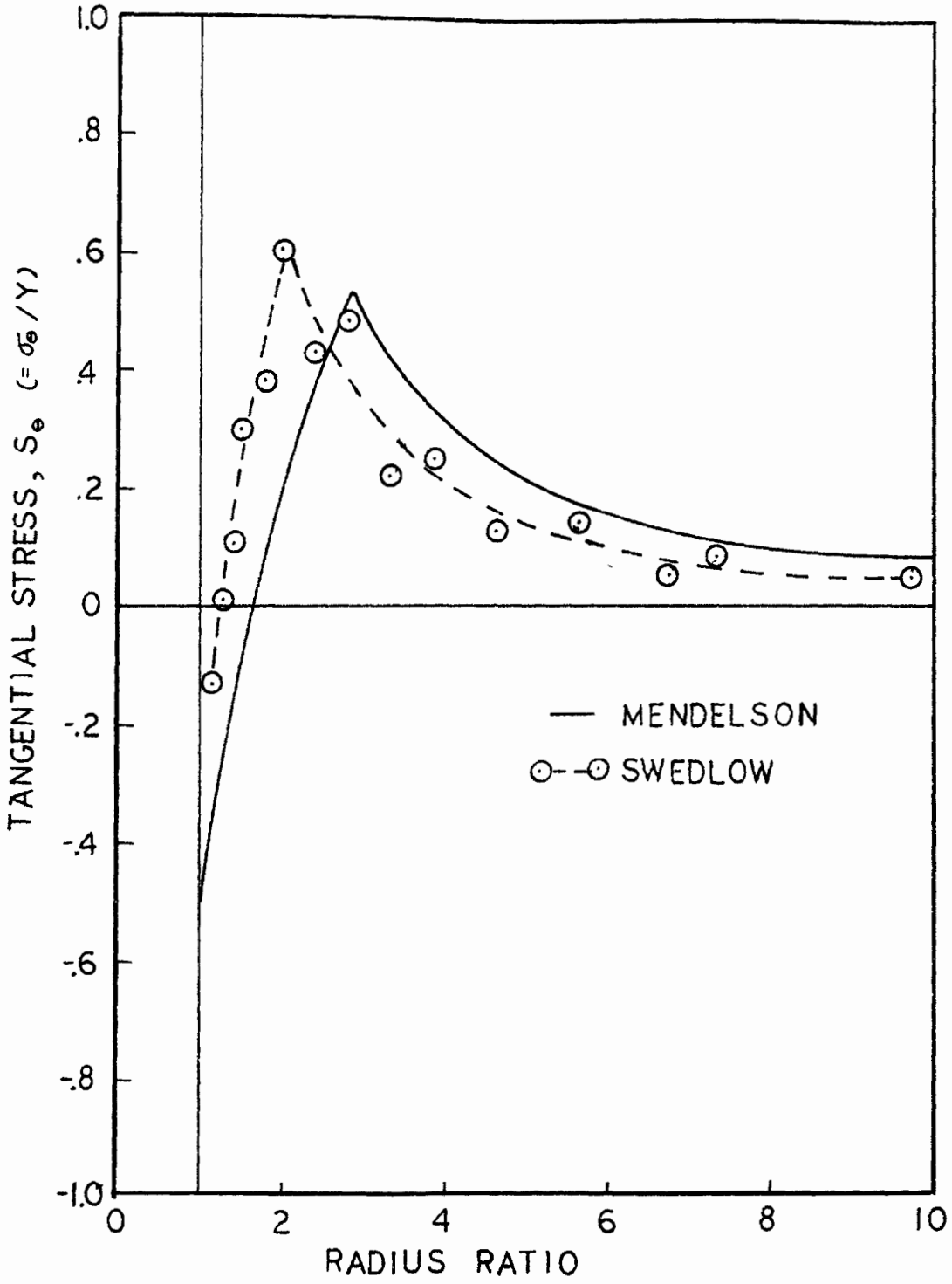

TANGENTIAL STRESS vs. RADIUS RATIO
THICK-WALLED CYLINDER, P=1.50

FIG. 14

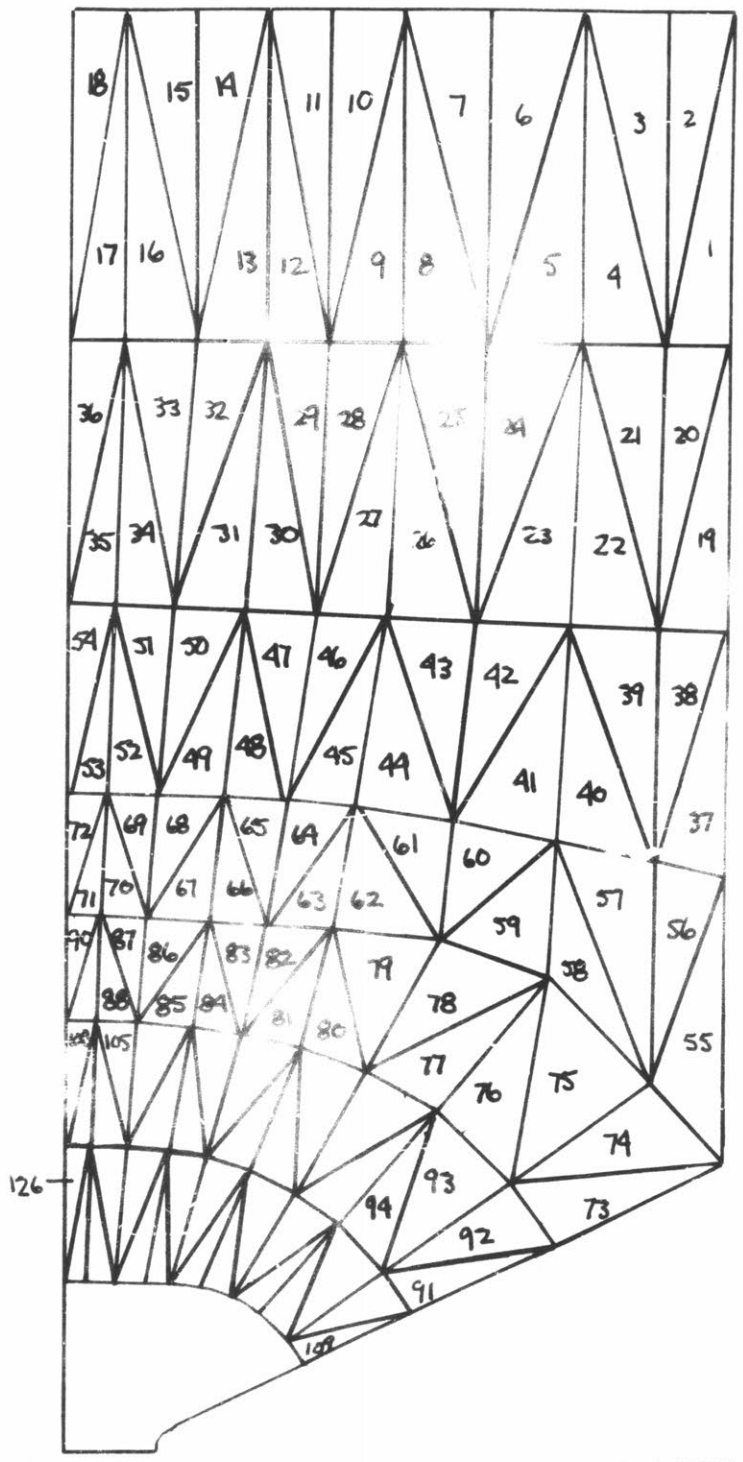

52° NOTCHED TENSILE SPECIMEN
FIG. 15-A. QUADRANT

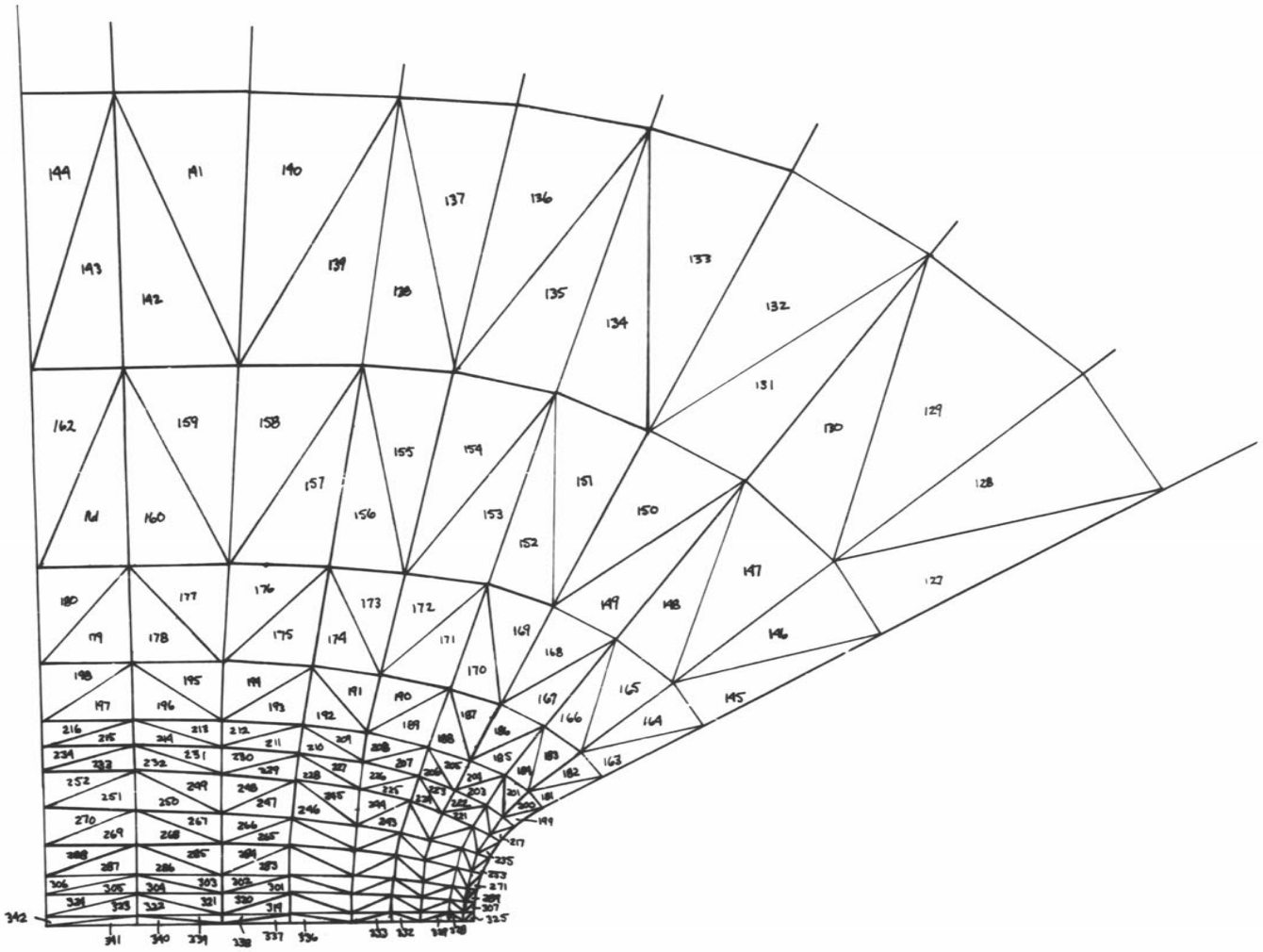

52° NOTCHED TENSILE SPECIMEN
FIG. 15-B. INSERT

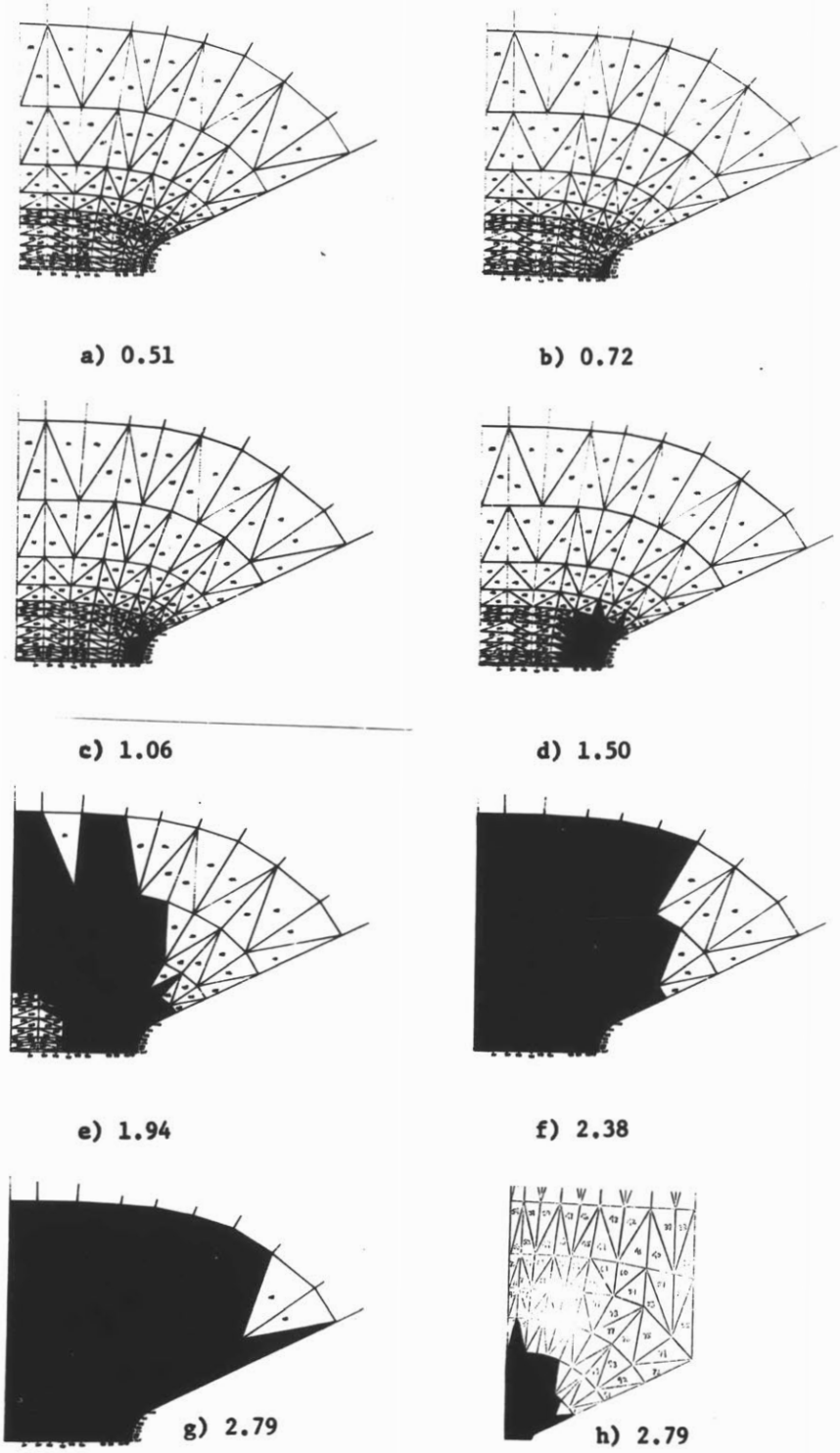

a) 0.51 b) 0.72

c) 1.06 d) 1.50

e) 1.94 f) 2.38

g) 2.79 h) 2.79

GROWTH OF PLASTIC ZONE IN 52° NOTCHED TENSILE SPECIMEN, FIG. 16

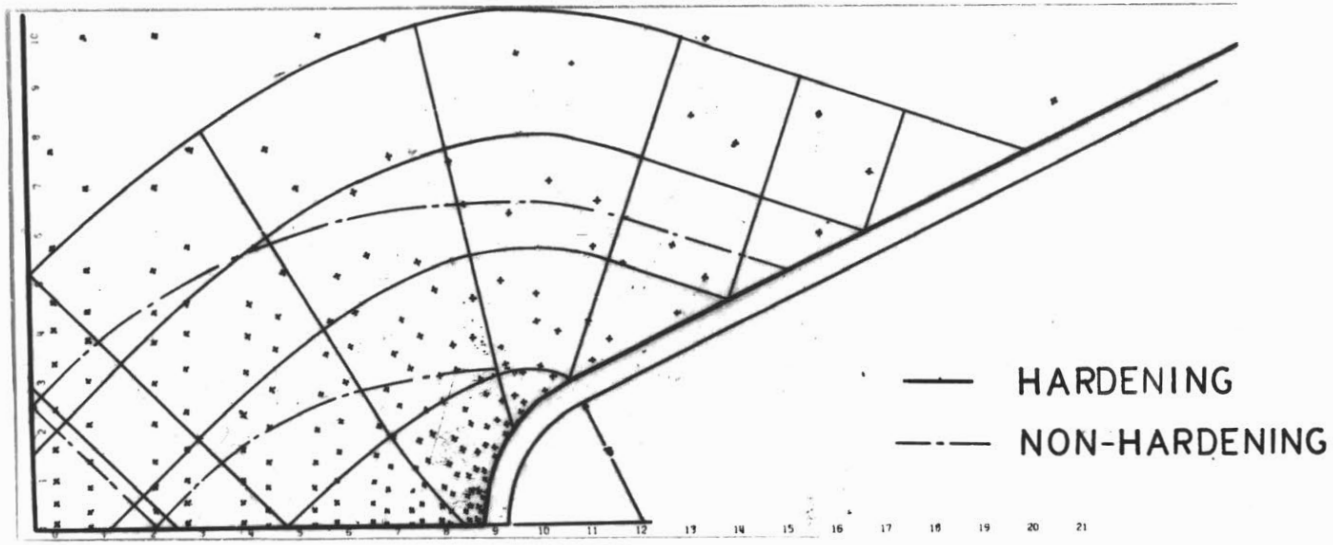

SLIPLINE FIELD FOR 52°
NOTCHED TENSILE SPECIMEN, $\sigma_\infty = 2.79$
FIG. 17

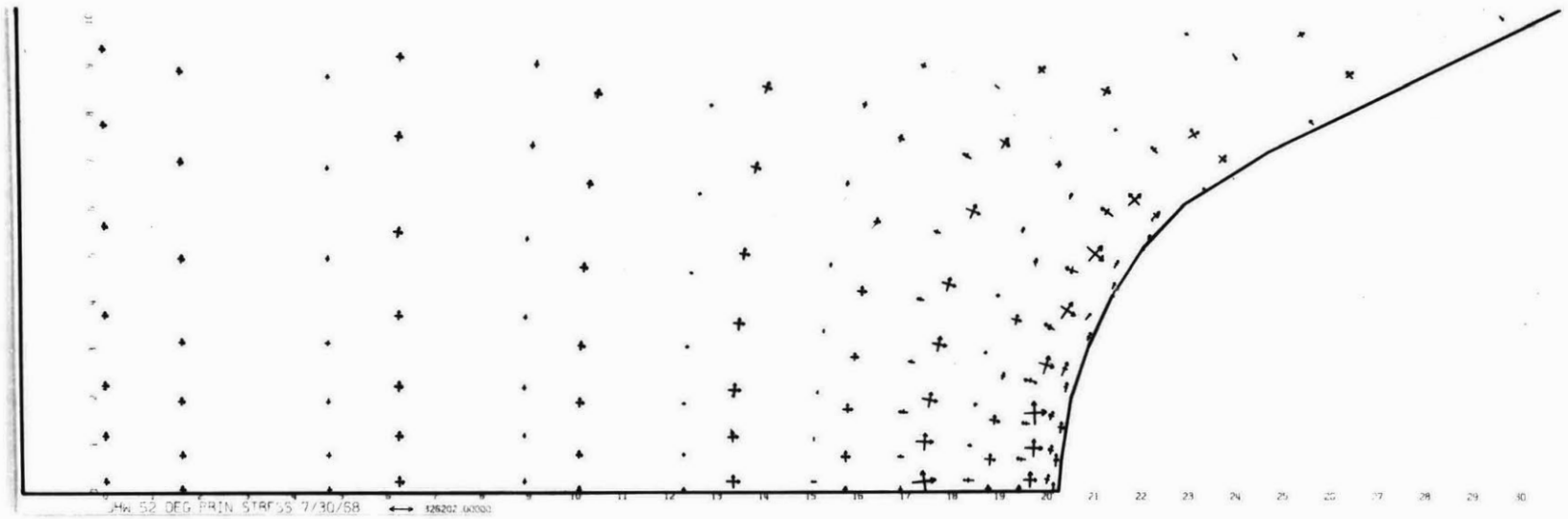

PRINCIPAL STRESSES FOR 52°
NOTCHED TENSILE SPECIMEN, $\sigma_\infty = 2.79$
FIG. 18

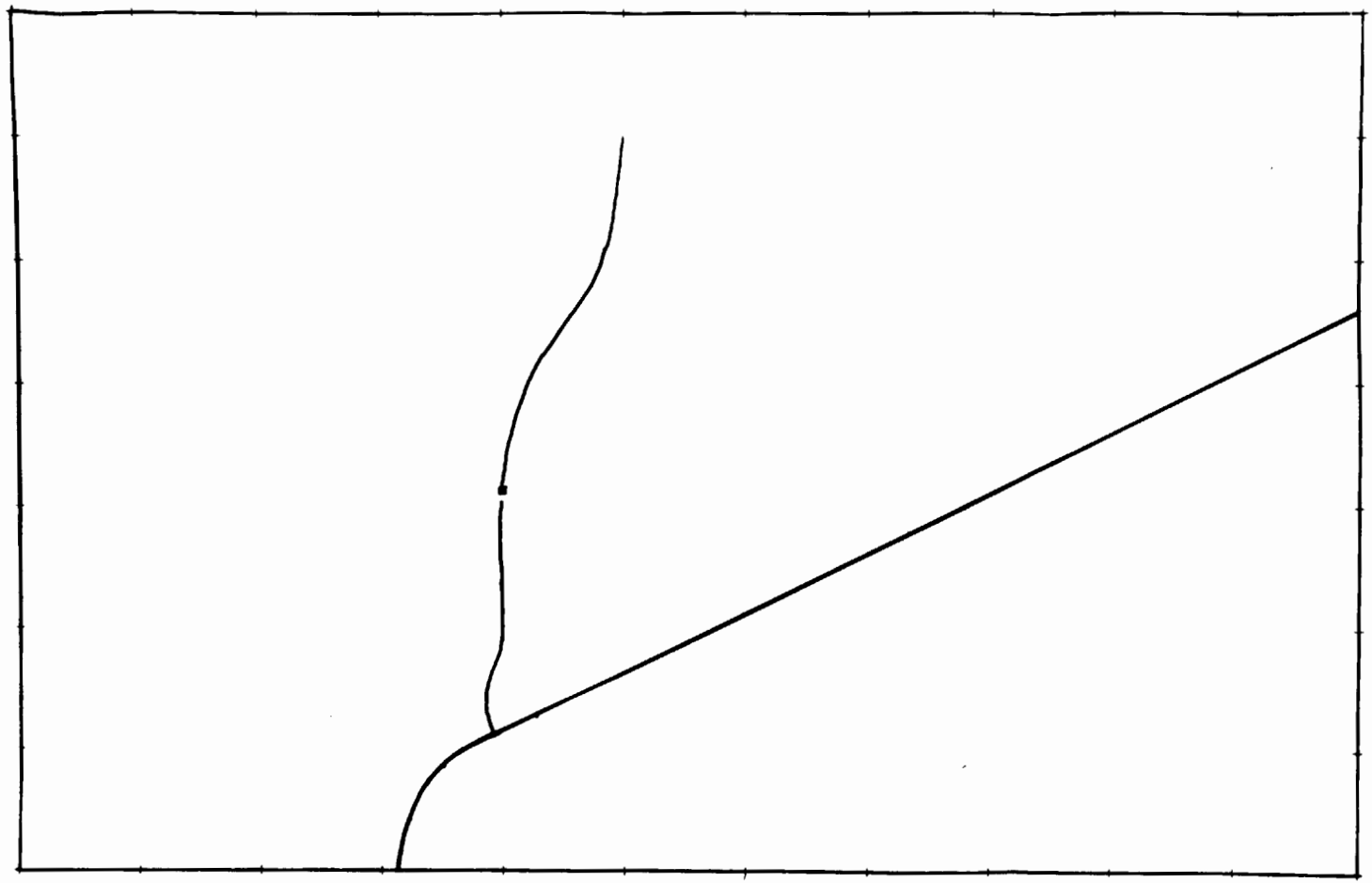

REGION OF YIELD FOR 52°
NOTCHED TENSILE SPECIMEN, $\sigma_\infty = 2.79$
FIG. 19

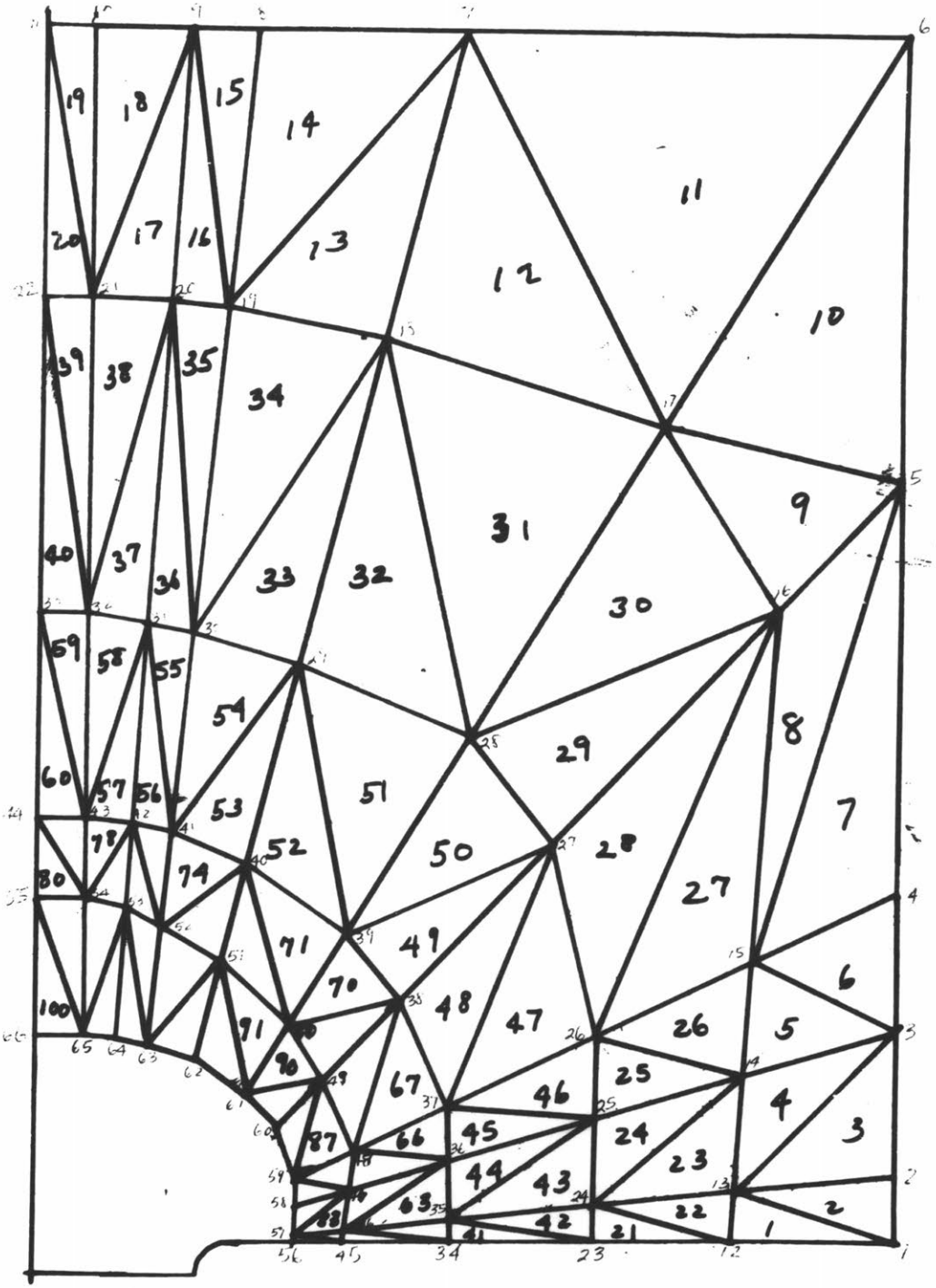

0° NOTCHED TENSILE SPECIMEN
FIG. 20-A. QUADRANT

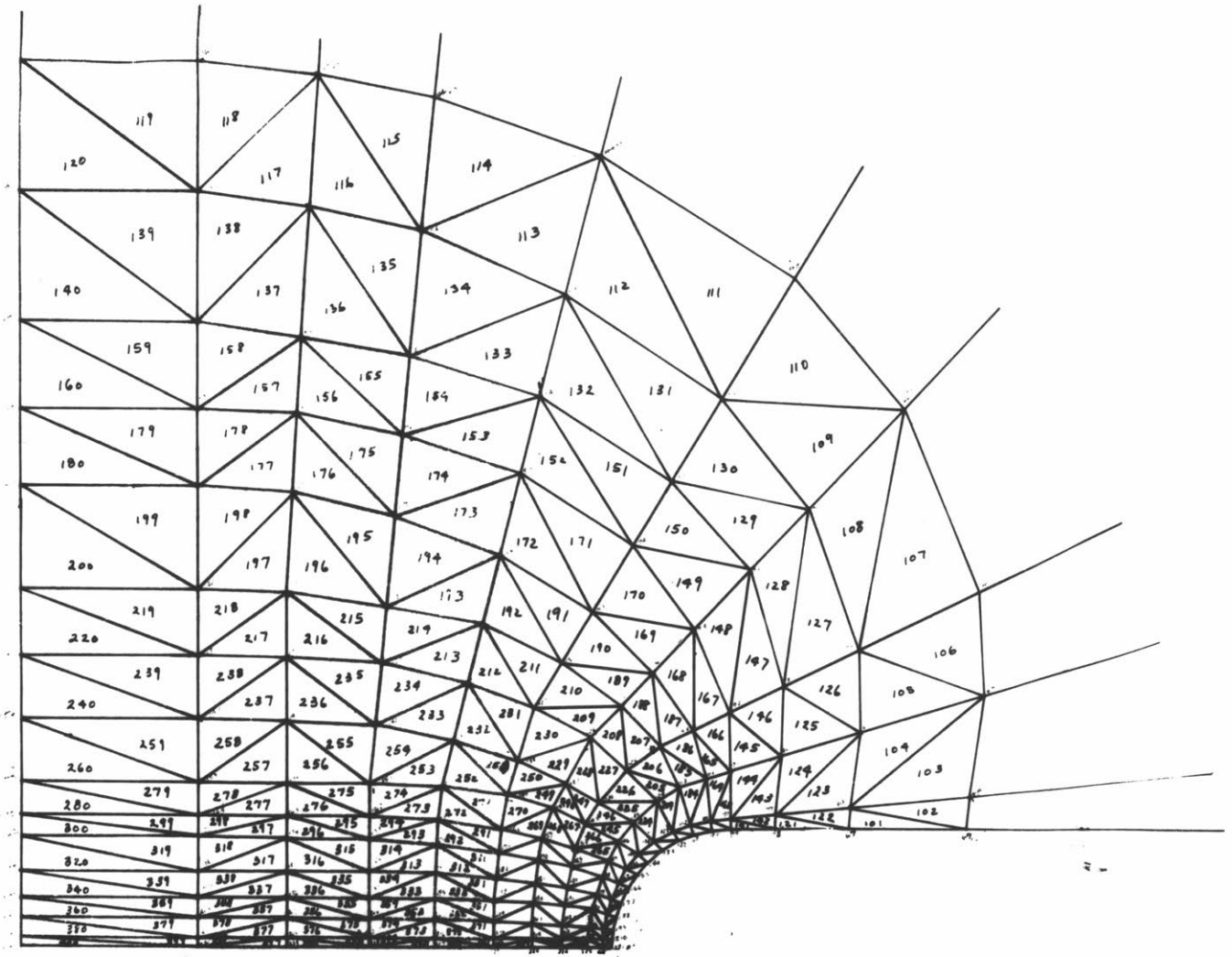

0° NOTCHED TENSILE SPECIMEN
FIG. 20-B. INSERT

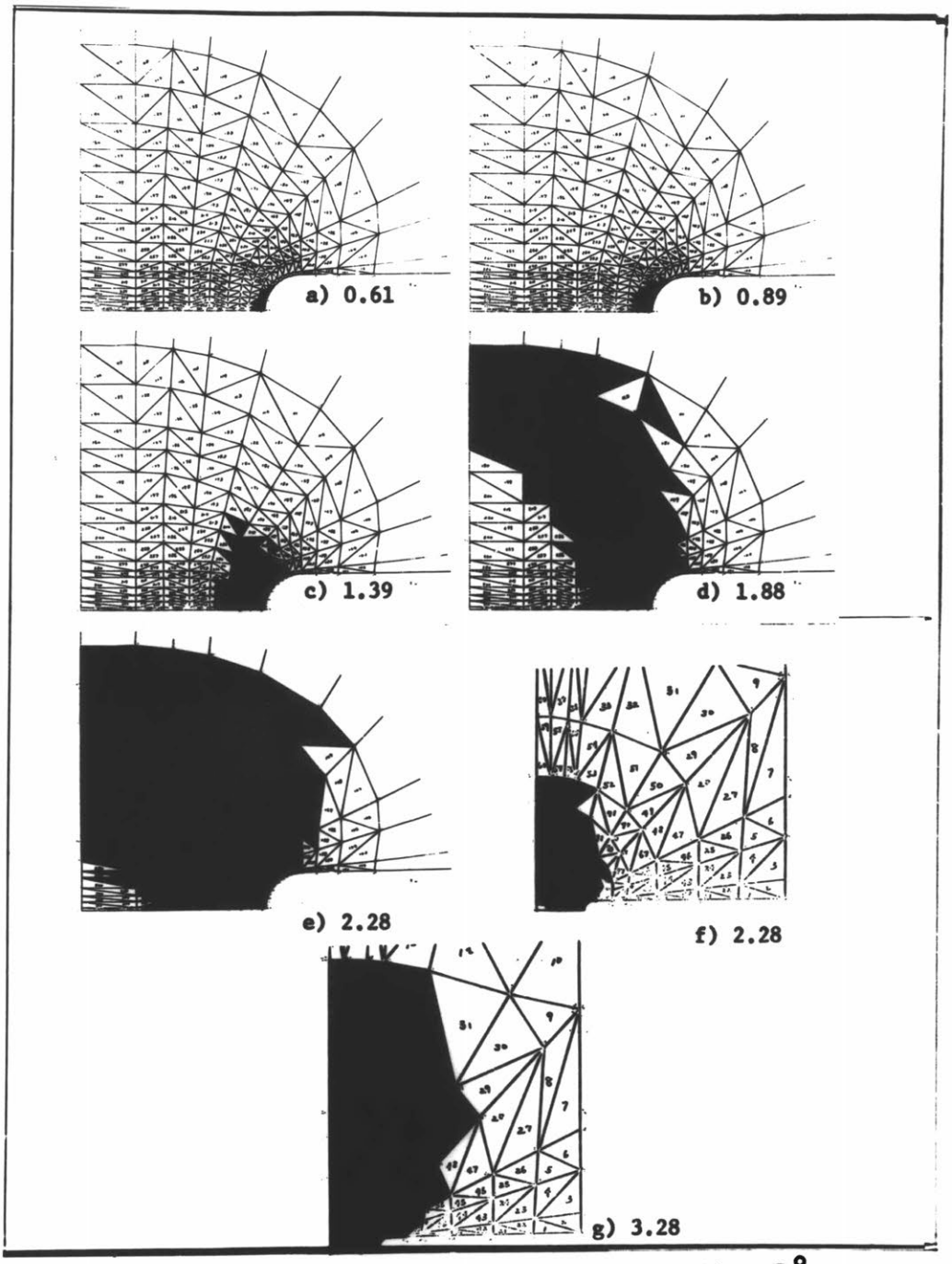

GROWTH OF PLASTIC ZONE IN 0° NOTCHED TENSILE SPECIMEN

FIG. 21

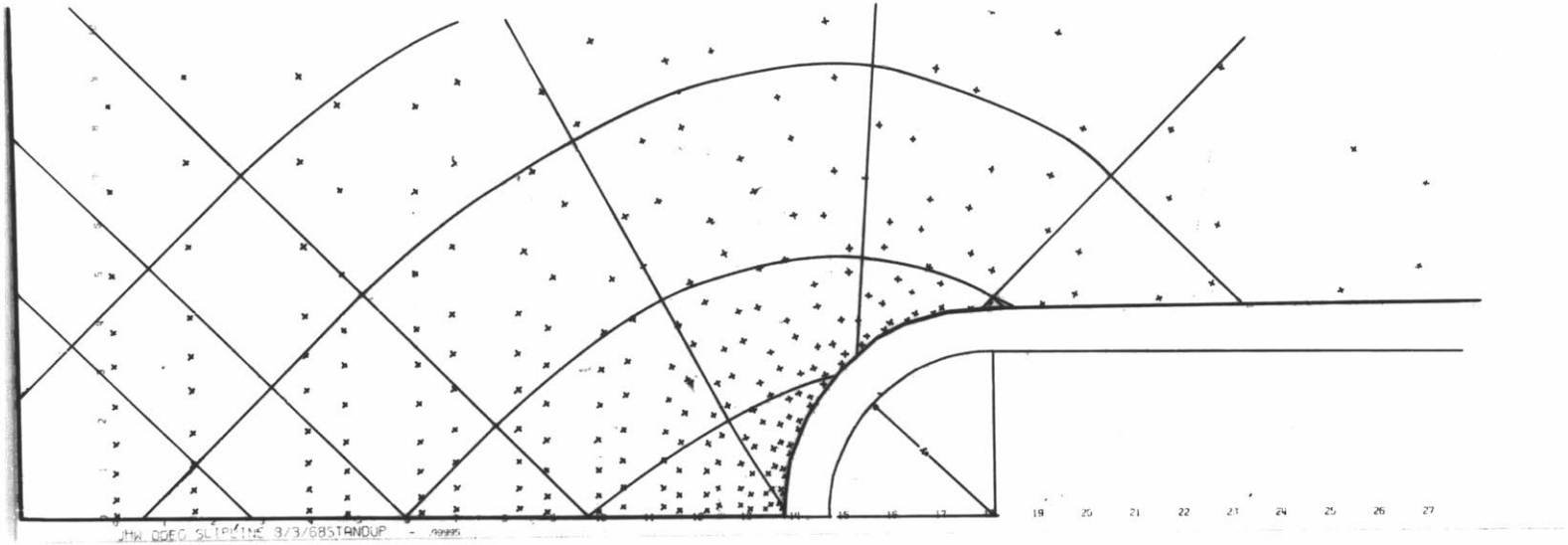

SLIPLINE FIELD FOR 0°
NOTCHED TENSILE SPECIMEN, $\sigma_\infty = 2.98$
FIG. 22

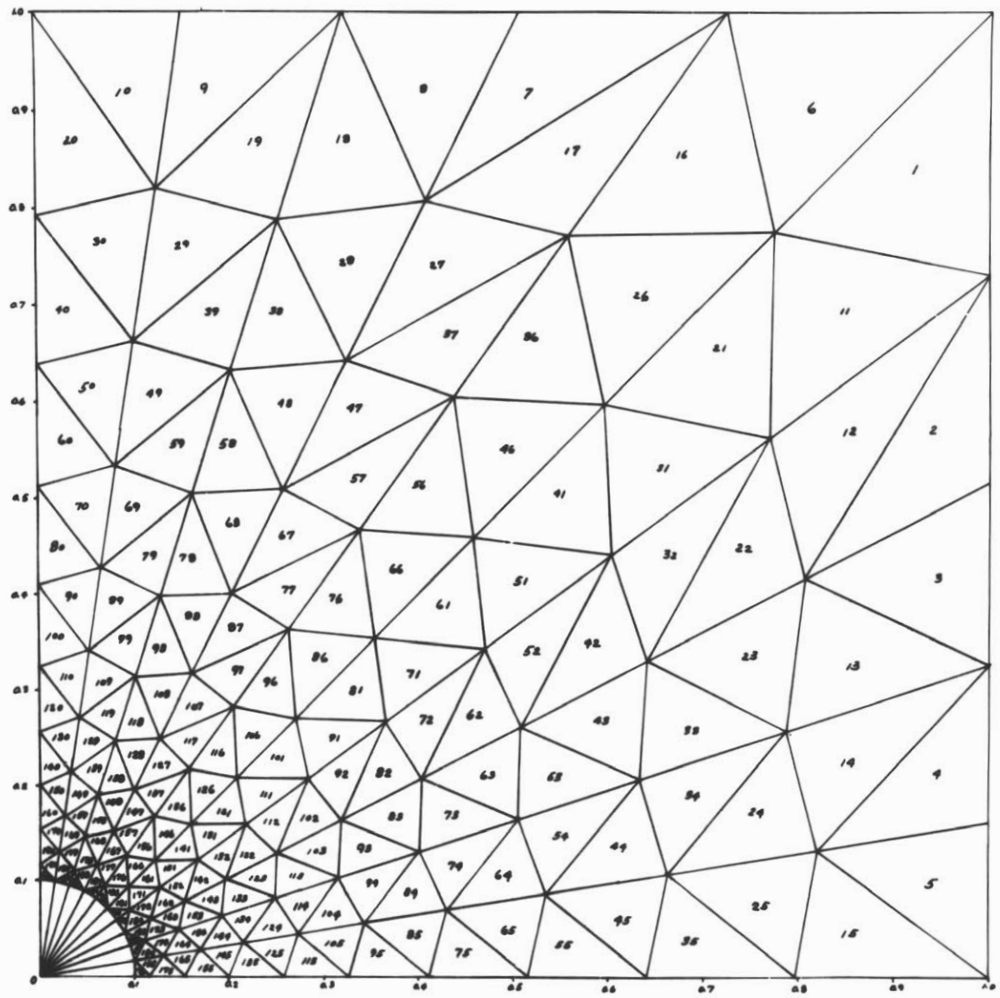

SQUARE PLATE WITH CENTER HOLE QUADRANT
FIG. 23

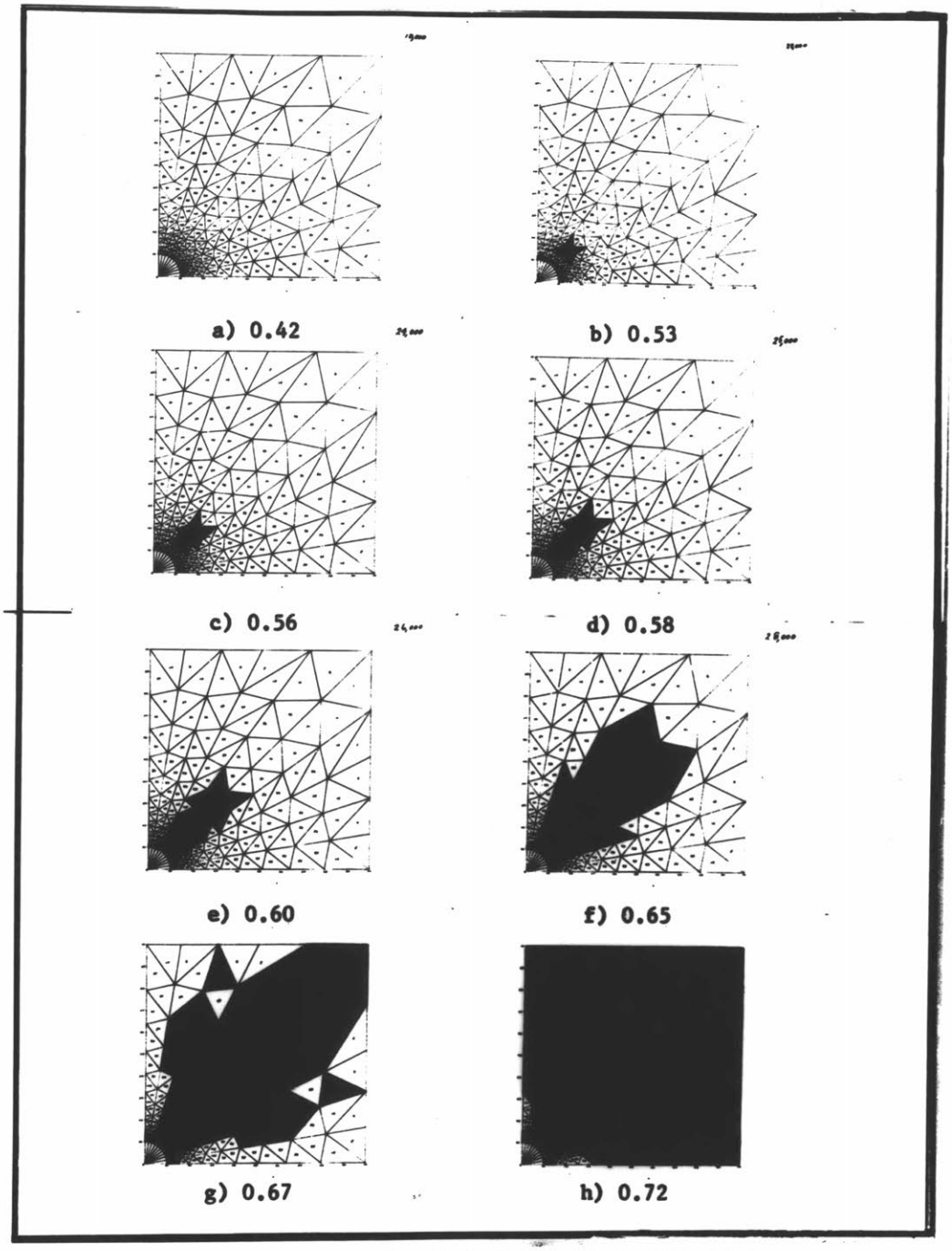

GROWTH OF PLASTIC ZONE IN
SQUARE PLATE WITH CENTER HOLE
FIG. 24

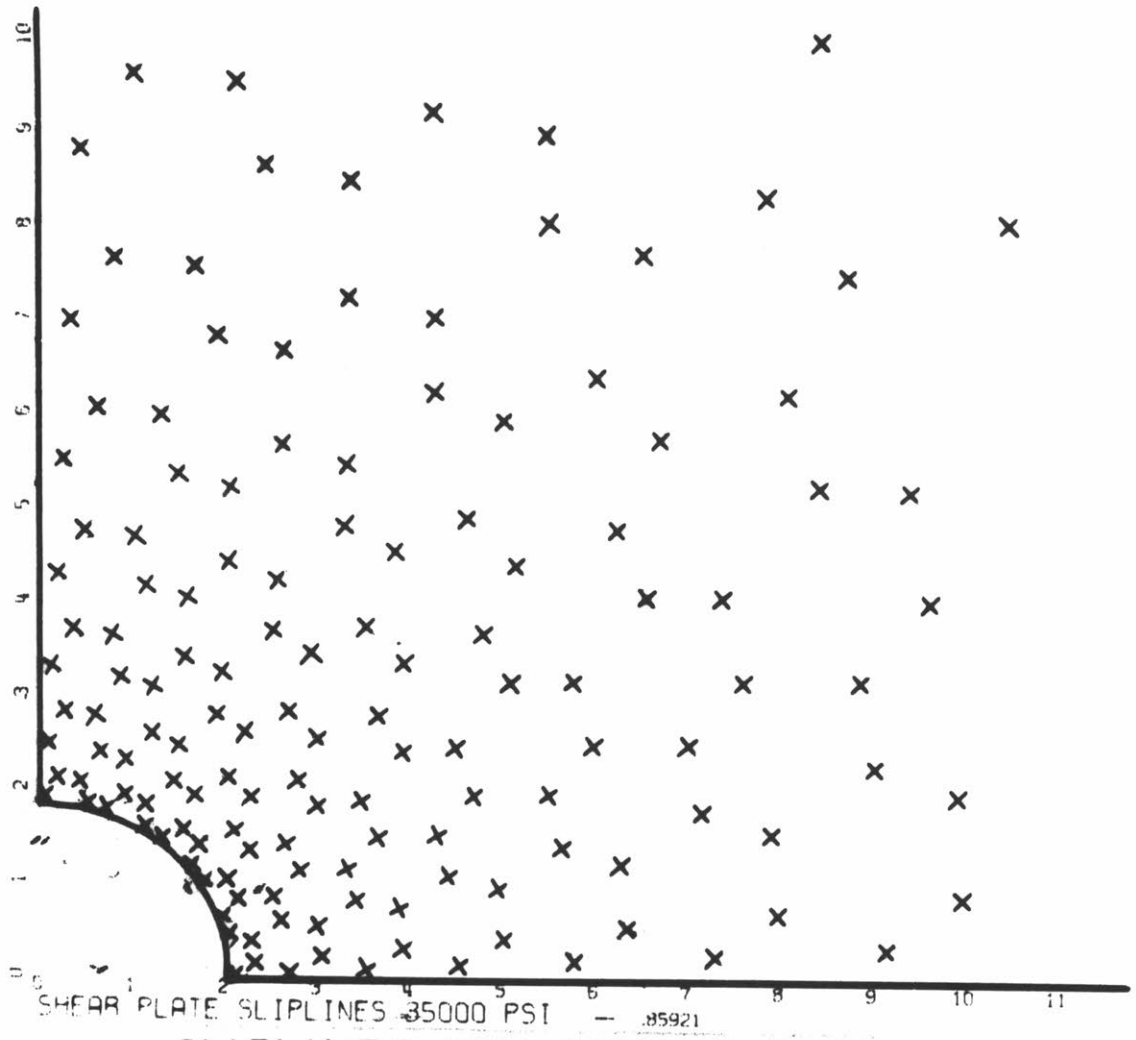

SLIPLINES FOR SQUARE PLATE WITH CENTER HOLE, $\sigma_\infty = .81$, FIG. 25

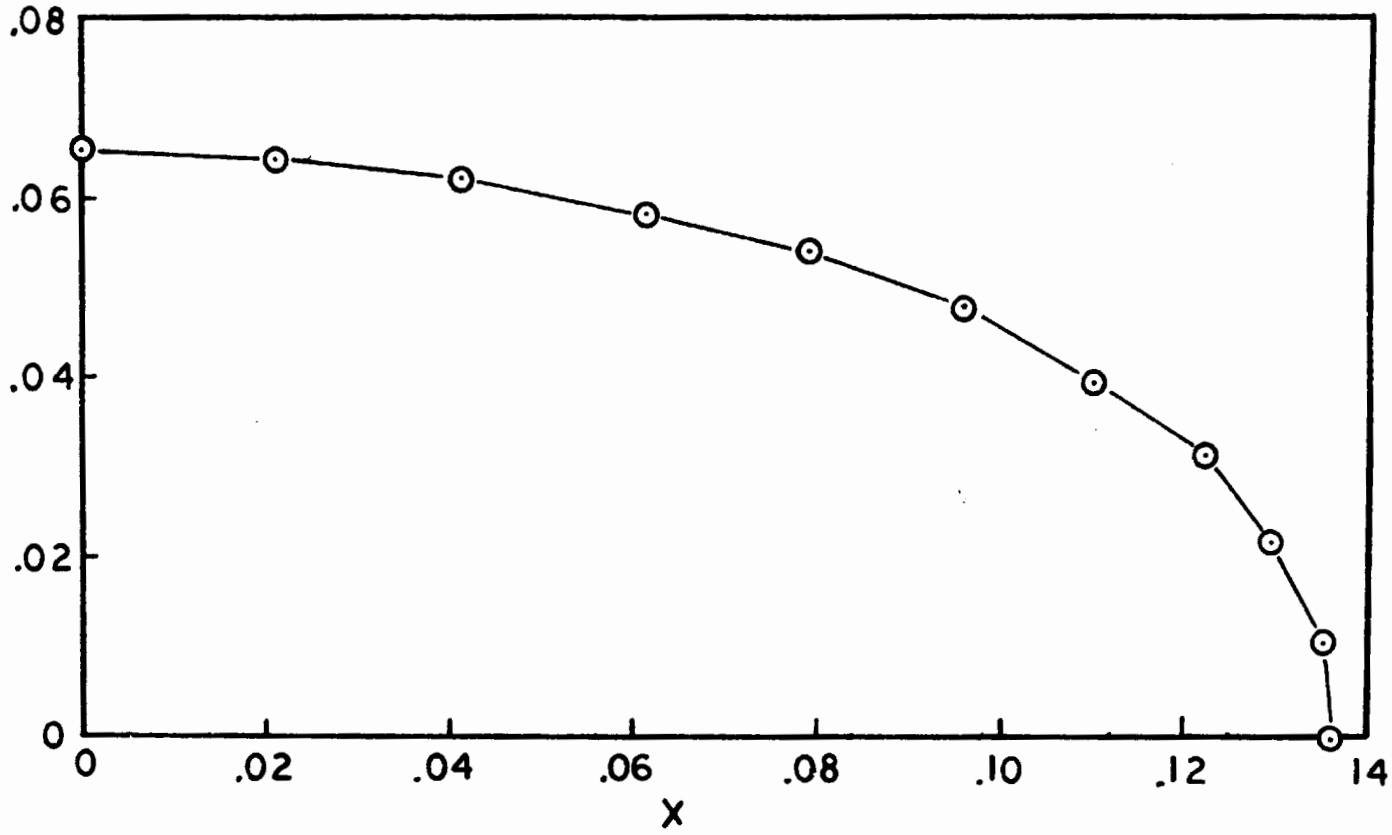

SHAPE OF CENTER HOLE
SQUARE PLATE PROBLEM, $\sigma_\infty = 1.14$
FIG. 26

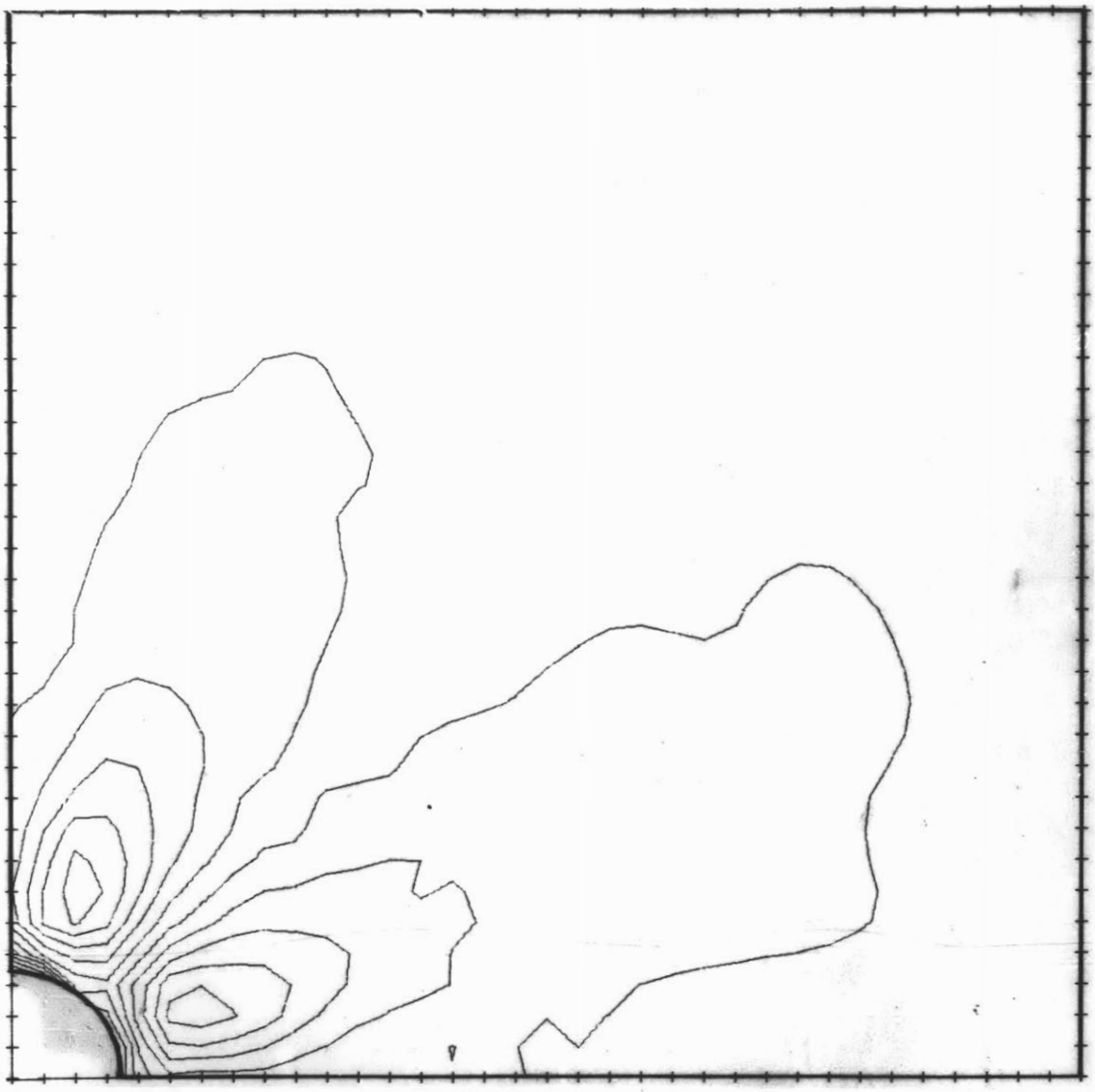

ISOCLINICS FOR SQUARE PLATE
WITH CENTER HOLE, $\sigma_\infty = 0.38$
FIG. 27

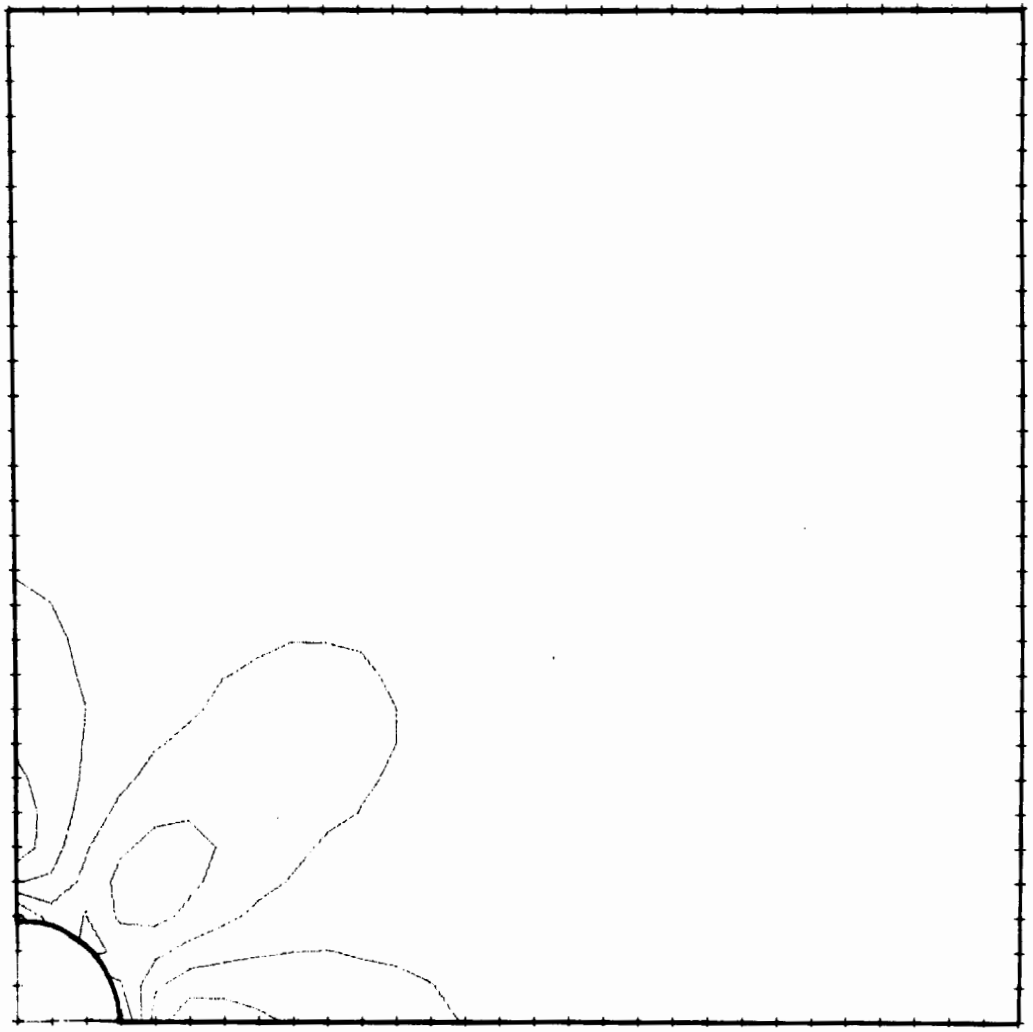

ISOCHROMATICS FOR SQUARE PLATE
WITH CENTER HOLE, σ_∞=0.38, FIG. 28